# Deliverable

## D4.4 Development of RRE forecasting services in OpenQuake

| Deliverable information | |
|---|---|
| **Work package** | WP4 Effects |
| **Lead** | [UNINA] |
| **Authors** | Y. Reuland, IBK-ETH<br>L. Bodenmann, IBK-ETH<br>N. Blagojevic, IBK-ETH<br>B. Stojadinovic, IBK-ETH |
| **Reviewers** | [Iunio Iervolino (UNINA), Pasquale Cito(UNINA), Mabel Orlacchio(UNINA), Eugenio Chioccarelli (UNINA), and Adriana Pacifico (UNINA)] |
| **Approval** | [Management Board] |
| **Status** | [Final] |
| **Dissemination level** | [Public] |
| **Delivery deadline** | 28.02.2022 |
| **Submission date** | [15.03.2022] |
| **Intranet path** | [DOCUMENTS/DELIVERABLES/File Name] |



This project has received funding from the European Union's Horizon 2020 research and innovation programme under grant agreement No 821115

# Table of contents

## Summary

This deliverable describes the recovery forecasting services made with a regional recovery simulation plug-in, named OQ-RRE (OpenQuake Recovery and Rebuilding Effort), that extends the earthquake scenario damage calculator in OpenQuake with repair and recovery prediction capabilities. Thus, the report encompasses:

- Suitable choices for recovery function meta-data and operators of post-earthquake recovery.
- A set of prototype recovery functions implemented to enable the development of a RRE (Recovery and Rebuilding Effort) forecasting model.
- The input files required to run the recovery plug-in and the created output files.
- A demonstrator of the plug-in capacities.

The deliverable further describes the developed RRE forecasting model and the predicted resilience quantification. Post-earthquake recovery data from the Kraljevo 2010 earthquake is used to compare recovery predictions with observed post-earthquake recovery.

## 1. Introduction into RRE

Damaging earthquake events carry the threat of widespread damage and loss to the built environment. In addition to direct human and economic losses, strong ground motions damage and weaken the built environment, potentially leading to buildings losing the capacity to safely harbour the functions they are intended for, such as housing or economic production. Thus, the main goal of recovery predictions is to predict the time that will be required to get back to 'normal', meaning pre-earthquake, levels of functionality (EERI, 2016). Indeed, the disruption of functionality due to damaging earthquakes may have negative and long-lasting effects on residents (Potter et al., 2015) and businesses (Cremen et al., 2020). In this perspective, the time that is required to re-establish pre-earthquake levels of functionality generates indirect losses that scale with the duration of repair and recovery efforts (RRE). While earthquake early warning (Böse et al., 2022) offers real-time alerts to reduce the impact of earthquakes and structural health monitoring (Reuland et al., 2021) has the potential to assess building-specific damage in near-real time, RRE operates on longer time scales, with full recovery potentially requiring several years.

The recovery predictions start where traditional risk assessment stops: downtime not only depends on the damage inflicted by the earthquake, but also on the duration until buildings are repaired. Downtime estimations are one of the most challenging loss assessment studies, as they involve many factors, some of which depend on community-level recovery impeding factors, such as damage inspection or repair financing, while other are building-specific, such as debris-removal and repair time. The recovery needs depend directly on the amount of damage sustained by a building during an earthquake and thus, RRE directly depend on the physical vulnerability of communities hit by earthquakes.

Several models have been developed to express the vulnerability of buildings at regional scale (Crowley, Despotaki, et al., 2021; Martins & Silva, 2021). In addition, computation tools for regional risk analysis and loss assessment have been developed, such as OpenQuake (GEM, 2022) and SELENA (S. Molina et al., 2010). However, reliable recovery prediction models for regional RRE are still under development. Burton et al. (2015) proposed recovery limit states, which describe the type and number of actions that are required to recover several functionality levels, based on classical fragility curves. Alisjahbana et al. (2020) proposed a stochastic queuing model for recovery services in order to predict realistic recovery trajectories that account for sequencing recovery activities. A review of existing approaches to analyze earthquake-induced loss of functionality can be found in M. W. Mieler et al. (2017).

Building-level methodologies have been developed to predict repair efforts; many are based on the PEER performance-based earthquake engineering paradigm (Cornell & Krawinkler, 2000; Moehle & Deierlein, 2004). Such probabilistic assessment methods for dynamic nonlinear analysis of component-level damage and repair needs have been anchored in the FEMA P-58 guidelines (FEMA, 2018). Recently, more refined methods have been proposed to predict building-specific repair needs with construction-management techniques for realistic repair-work sequencing (Terzic & Kolozvari, 2022) and to define more refined recovery targets, such as shelter-in-place (C. Molina et al., 2022).

While such building-specific analysis tools enable precise predictions of repair efforts conditional on intensity measures, simplified methods are required to predict regional RRE. In addition, downtime is not limited to the time required to remove debris and repair damaged components. Several impeding factors precede the actual repair works, such as inspection of the building, engineering assessment of the damage and design of adequate repair measures, as well as finding and financing a contractor (Almufti & Willford, 2013). These impeding factors are not building-specific, but depend on the preparedness and resourcefulness of the entire community hit by an earthquake (Bruneau et al., 2003).

The supply of these recovery services, which are required for damaged assets to regain their functionality, are limited, especially in the aftermath of a damaging earthquake, when many buildings potentially lost functionality. The iRe-CoDeS (Interdependent Resilience Compositional Demand/Supply) quantification framework (Blagojevic, Didier, et al., 2021a; Didier, Broccardo, et al., 2018) has been extended to evaluate the influence of constrained supply of recovery services on the ability of communities to bounce back (Blagojevic et al., 2021b). This compositional demand and supply resilience quantification framework relies on a bottom-up simulation of the attribution of a limited amount of supply of recovery services, such as inspectors and workers, to assets that need, or have an open demand for, such recovery actions. While this simulation framework offers the capabilities to simulate the inter-dependencies of several networks, such as electricity, telecommunication, and transportation, this level of information is often lacking in real-world applications.

This report starts with a description of suitable regional functions of repair and recovery efforts for residential buildings (Chapter 2). Then, the components of the recovery plug-in for OpenQuake are presented in Chapter 3 and demonstrated on a fictitious case study (Chapter 4). Chapter 5 contains the validation with reported RREs after the 2010 Kraljevo earthquake and a description of ways to improve recovery predictions through dynamically improving the precision of the spatial distributions of damage predictions. Finally, Chapter 6 contains summary, conclusions, and limitations of the OQ-RRE forecasting services.

**Open science and code sharing**

Owing to the ever-growing conscience of the benefits of open science, a stable version of the OQ-RRE calculator will be made publicly available under a creative-commons license, after successful testing and compilation of a user manual, before the end of the RISE project.

**Integration within the RISE project**

Within WP4 Task 4.3, a model to compute the time-demand of RRE in near real-time is developed, validated and verified, in order to enable RRE forecasting. This regional RRE forecasting model is provided in the form of an OpenQuake RRE prediction plug-in, called OQ-RRE, and demonstrated by extending the OpenQuake earthquake scenario damage engine towards RRE simulation based on the iRe-CoDeS compositional framework, thus providing rapid post-earthquake estimations of RRE and resilience quantification.

With the estimation of RRE, the effects of earthquakes, treated in WP4, get the additional dimension of time by extending assessment of direct losses, often predicted by rapid loss assessment, to the time – required by a community hit by an earthquake – to recover pre-earthquake levels of functionality.

Time-varying vulnerability of buildings during long-term and short-term sequence of earthquakes is influenced by state-dependent fragility, which involves damage accumulation analyzed in WP4 Task 4.2. However, the post-earthquake community-level vulnerability also depends on the duration of repair efforts on damaged buildings, and thus, RRE predictions contribute to time-varying seismic risk predictions.

Given the scope of RISE covers rapid post-earthquake predictions, the developed OQ-RRE plug-in is limited to recovery predictions for scenario earthquake simulations and does not allow for fully probabilistic risk and consequence predictions. The limited scope of the available post-earthquake recovery data circumscribed the extent of the developed OpenQuake plug-in validation. Yet, verification and validation has been performed using the 2010 Kraljevo post-earthquake recovery data.

## 2. From repair to recovery

Repair efforts include all the actions required to repair the damage inflicted to a given asset by an earthquake. Structure-specific predictions of repair time and cost have been proposed in the past and usually involve a bottom-up methodology deriving the repair needs for individual components of a structure. Based on the performance-based earthquake engineering (PBEE) framework (Moehle & Deierlein, 2004), the FEMA P-58 framework makes use of component-level damage predictions that are related to repair efforts, such as number of worker-hours and repair costs. Silva et al. (2020) proposed a methodology to adapt the FEMA framework for cost-estimates outside the US, for which the cost values have been calibrated. As such bottom-up methods cannot be implemented for all buildings, HAZUS guidelines (FEMA, 2004) provide median repair time and cost based on the global damage state of a building.

However, the downtime, or time to recover an asset, is not limited to the repair time, as several impeding factors need to be met before the actual repair works can start. These impeding factors, also referred to as irrational delays (De Iuliis et al., 2019), may include inspection, engineering assessment and design, contractor mobilization, permitting, and financing. The total downtime is essential to estimate indirect financial losses such as business interruption, whose high dependency on the building function undermines it evaluation at regional scale.

The REDi (Resilience-based Earthquake Design Initiative) framework (Almufti & Willford, 2013; M. Mieler et al., 2018) introduces three levels of recovery targets:

- re-occupancy is reached when the building is deemed sufficiently safe to be used for shelter;
- functional recovery is reached when a building is re-occupiable and external utilities (such as electricity, water, and gas) are available;
- full recovery is reached when a building is re-occupiable, functionally recovered and all structural and non-structural elements have been repaired, even if they require only cosmetic repair measures.

This report focusses on the housing supply provided by residential buildings. Therefore, the recovery state of interest is re-occupancy, which offers safe shelter to the building inhabitants. While it is reasonable to assume that building inhabitants do not require immediate functional recovery, the acceptable duration without external utilities may not be unlimited. However, the time to restore external utilities typically remains low in developed countries, as evidenced by the suggested values contained in the REDi framework. Molina et al. (2022) proposed additional recovery

states: stability and shelter-in-place, for which the building does not need to be repaired to pre-earthquake requirements regarding structural safety. However, this report does not include this reduced structural safety levels.

In this chapter, a method to derive the efforts that are required to repair a building to the re-occupancy level of functionality is presented. Then, impeding factors that govern the recovery process are outlined. Finally, the Re-CoDeS framework, which allows the regional simulation of recovery trajectories and thus, the resilience of a region with respect to earthquakes, is presented.

## 2.1 Earthquake consequence model – Repair time

The FEMA P-58 framework (FEMA, 2018) contains a performance assessment calculation tool (PACT) that links performance states, defined as function of engineering-demand parameters (EDPs), with repair efforts. The PACT also contains economy-of-scale considerations that linearly reduce the time and money required to repair a single component – between a minimum and maximum bound - when multiple similar components need to be repaired.

Repair efforts include all the work steps that are required to bring structural (or non-structural) building components back to a healthy, pre-earthquake, state. For instance, in case of masonry walls with some diagonal cracks that remain closed (i.e., hardly noticeable crack widths of less than 1mm after the earthquake) would require grouting, epoxy injection, and painting to repair the damage (FEMA, 2019).

The repair efforts that are proposed by the PACT guideline aim at full recovery, thus also including minor repair works to reach full recovery. However, according to the REDi framework, re-occupancy does require all structural and non-structural elements to be repaired, as this level of functionality mostly requires a building to provide safe shelter for the inhabitants.

While such building-specific analysis of repair needs is relevant to reach performance goals when designing and retrofitting buildings, a simplified analysis is required to assess repair efforts for regional building stocks. As shown in Table 1, average clean-up and repair times are provided by HAZUS manual (FEMA, 2004) as a function of the level of damage sustained by a building. These values represent median values and apply to the North-American building stock. While the same documentation also provides values for downtime and business interruption, it should be noted that, unlike repair, these values have a strong regional correlation, as they depend on preparedness and other socio-economic indicators.

**Table 1 Clean-up and repair time from the HAZUS documentation for typical residential buildings.**

| Building type | Slight damage | Moderate damage | Extensive damage | Complete damage |
|---|---|---|---|---|
| Single Family Dwelling | 2 | 30 | 90 | 180 |
| Multi Family dwelling | 2 | 30 | 120 | 240 |

### Example of building-specific derivation of repair time

As stated before, the median repair time values of the HAZUS manual are established for typical American buildings. Therefore, we analyze a typical Swiss unreinforced masonry building, built in 1955, with stiff reinforced-concrete floor slabs (more information can be found in Karbassi & Lestuzzi (2014), where the building is labelled YVR14).

An incremental dynamic analysis (Vamvatsikos & Cornell, 2002), following the principles outlined by Vamvatsikos (2011), is performed on a three-dimensional model of the structure. For each nonlinear time-history analysis, the damage state is established for all the elements (i.e., walls)

based on damage-state thresholds (Didier, Abbiati, et al., 2018; FEMA, 2019). The drift values for each wall are derived from the relationship between inter-story drift and element-drift, based on a static nonlinear pushover analysis of the building. The derivation of an overall floor-level damage state, which governs the decision whether repair is required to reach re-occupancy, is obtained through averaging the damage states of all walls of a given floor (Almufti & Willford, 2013).

Our objective for RRE lies in the functional recovery state of re-occupancy, therefore esthetical repair actions, such as repainting, are ignored. The repair time for each damaged element is calculated based on the damage state and the repair time proposed by the PACT (FEMA, 2019).

The predicted repair duration exceedance probability, expressed in terms of repair effort measured in worker-days, for slight, moderate, and extensive damage states of the YVR14 building, are shown in Figure 1. The global damage states are derived from the idealized bilinear pushover curve and follows the suggestions of the SERA project and (Villar-Vega & Silva, 2017).

Overall, the median values proposed by the HAZUS manual are realistic, given they were developed for the North American building stock. The slight and moderate damage HAZUS estimates are reasonably close to the median of the YVR14 repair duration distribution, while the repair duration for extensive damage is in the tail of the distribution and overestimates the repair efforts for the Swiss masonry building.

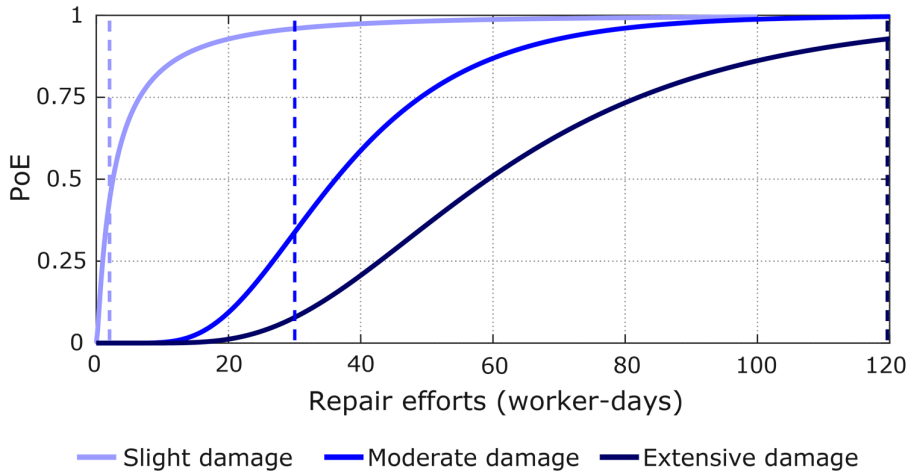


**Figure 1 Distribution of the probability of exceeding repair time duration for slight, moderate, and extensive damage of a residential unreinforced masonry building. Repair time from HAZUS for multi-family dwellings is shown as dashed lines for comparison.**

In addition to the median values proposed by HAZUS (reported in Table 1), empirical observations of repair times for damaged buildings from past earthquake events are another source of repair effort and cost estimates (e.g., Kappos et al. (2007), Stojadinovic et al. (2017)). Based on the return of experience of experts involved in the post-earthquake recovery after the 2010 Kraljevo (Serbia) earthquake (Blagojević et al., 2021; Marinkovic et al., 2018, 2019; Seismological Survey of Serbia, 2010; Stojadinovic et al., 2021), repair duration has been obtained for single-family and multi-family dwellings (see Table 2). The single-family buildings are generally limited to one floor, while multi-family buildings comprise several floors. Generally, the repair efforts derived from the number of workers and the duration of their activity, is compatible with the median values provided by HAZUS, reported in Table 1. A major difference can be found for the repair efforts of slightly damaged multi-family buildings, which require 35 to 70 worker days, while a median value of 2 is proposed by HAZUS (see Table 1), pointing to a stark difference in typical building typologies assumed by HAZUS (for the US) and the actual building typologies in the earthquake-affected region.

**Table 2 Repair efforts established on empirical values from the Kraljevo 2010 earthquake. Repair efforts are deduced from number of workers and repair duration intervals.**

| Building function | Damage State | Number of workers | Repair Duration (days) | Repair efforts (worker-days) |
|---|---|---|---|---|
| Single-family residential | Slight | [1, 2] | [4, 5] | [4, 10] |
| | Moderate | [2, 3] | [5, 7] | [10, 21] |
| | Extensive | [3, 6] | [7, 15] | [21, 90] |
| Multi-family residential | Slight | [5, 7] | [7, 10] | [35, 70] |
| | Moderate | [5, 10] | [7, 10] | [35, 100] |

## 2.2 Impeding factors

While the repair time estimates of HAZUS are found to be acceptable, the recovery time estimation highly depends on local conditions, preparedness, and resourcefulness of the affected region. The major difference between repair and recovery time lies in the impeding factors, also called irrational components of recovery, which delay the start of the actual clean-up and repair works. The most common impeding factors for earthquake-damaged buildings are:

- *Inspection*, also called visual screening, which is performed by trained building professionals that judge the severity of damage and attribute damage tags (such as the ATC-20 red, yellow, green classification) or directly damage states, for instance after the Kraljevo 2010 earthquake (Marinkovic et al., 2019). Inspection may be performed upon request of the building owner or performed by default in a given region, for instance the zone that exceeds a given macro-seismic intensity provided by a shake map.
- *Engineering assessment*, also referred to as detailed inspection, which may become necessary if the visual inspection fails to be conclusive or if a building owner requires additional inspection.
- *Repair design* requires building professionals, such as engineers, to elaborate a repair project for a damaged building. While RRE estimates typically consist in reaching pre-earthquake levels, repair may go beyond this performance goal and aim for safe and resilient buildings.
- *Financing* is required to ensure the building owner can pay for the repair works. The duration of this impeding factor may greatly vary based on socio-economic situation, governmental aid, and subscription of an earthquake insurance (Almufti & Willford, 2013).
- *Permitting* consists of getting the permission to carry out repair or replacement works. Depending on the local conditions, this may be a purely administrative act or involve a control of the repair design.
- *Contracting* describes the action of ensuring a contractor to carry out the repair works.

In addition to these impeding factors, other criteria may delay repair work, for instance a cordon that limits access to a part of the city (Underwood et al., 2020), disruptions of the transportation network due to damaged road-network components (Zhang & Alipour, 2020), or scarcity of resources in the aftermath of an earthquake (Costa et al., 2020). Given the complexity and correlation of these factors, they are omitted from this work.

Recovery impeding factors have a large dependency on local regulations and institutional decisions, as evidenced by the application-process for public funding after the 2009 L'Aquila earthquake (Di Ludovico et al. 2017a; Di Ludovico et al. 2017b). In addition, impeding factors are dynamic and can change based on the level of preparedness, for instance insurance or private savings may significantly speed up financing (Almufti & Willford, 2013; Burton et al., 2019). In addition, impeding factors depend on the damage level, the building ownership, and the building function. Finally, impeding factors may be reduced through specific policy decisions, such as relaxed permitting and waiving bidding rule for hurricane-damaged buildings (Wang & van de Lindt, 2021).

### 2.3 Recovery modelling using a compositional demand and supply model

While several models exist to predict recovery, we chose a bottom-up modelling technique that is based on the demand and supply of recovery services (Blagojevic et al., 2021a; Didier et al., 2018). Each damaged building has a recovery demand, that can depend on its properties (e.g., number of floors, occupancy type, socio-economic characteristics) and state of damage. Recovery of a building is simulated as a sequence of events, occurring in serial or in parallel, such as inspection, permitting and repair, where for each a duration, demand and preceding activities must be defined. For instance, inspection service demand is needed to inspect a building, while workers are needed to start building's repair (Blagojevic, Didier, et al., 2021b). However, repair works can only start if the demand for all impeding recovery factors, such as inspection, repair time, financing, and contracting, are met.

During the recovery simulation, available R/Ss are distributed among damaged buildings and only the buildings whose recovery demand is met are recovered. Such an approach is also capable of capturing components' functional interdependency and quantifying disaster resilience (Blagojevic, Hefti, et al., 2021).

Demand for recovery services from the community will arise for all impeding factors, described in the previous sections. In addition, social communities have a persistent demand for functional services, such as housing. A lack of resilience (LoR) is therefore observed when this service demand cannot be fully supplied, for instance, because a damaged building cannot provide housing services. The total LoR is the sum of un-supplied service over time, until recovery is reached.

### 2.4 Repair costs

In a manner similar to repair time, the HAZUS manual proposes repair cost estimates. While A. Silva et al. (2020) proposed a rational approach to transform the HAZUS repair-cost estimates from North American cost levels to other countries, empirical repair-cost functions have been established as well in Europe from past earthquakes, for instance by Kappos et al.( 2007) for the 1999 Athens earthquake and by del Vecchio et al. (2018) for the 2009 L'Aquila earthquake.

Typically, the repair cost is indicated in percentage of the replacement of the building cost – which is much more stable than building value – and thus, depends on the exposure model and the predicted damage states, which are covered by WP4 task 4.1.

## 3. Integrating recovery predictions into the OpenQuake framework

The OpenQuake (OQ) software provides a powerful tool to perform regional seismic hazard and risk calculations (GEM, 2022). While it provides capabilities for probabilistic hazard and risk analysis, we are focusing on damage predictions for a scenario earthquake. This choice is motivated by the focus of RISE being on rapid post-earthquake loss predictions.

Within task 4.3, a plug-in code has been developed to extend the OQ damage scenario capabilities towards RRE predictions. The structure of the OQ-RRE is shown in Figure 2. The plug-in takes as input the outcome of a damage scenario calculation, exported as a csv-file, and the exposure file, such as available from the ESRM2020 model. In addition, the information required to perform a compositional demand/supply resilience quantification following the iRe-CoDeS framework, such as the community housing or repair services supply levels, are required.

The plug-in transforms damage states, such as the HAZUS damage levels (none, slight, moderate, extensive, complete) into a range of recovery actions needed to regain functionality. As stated

before, the current version of the calculator and the repair functions are tailored to re-occupancy, which does not require functionality of external distribution networks, such as transportation, electricity, and wastewater. The recovery plug-in then performs predictions of recovery trajectory according to a simplified regional application of the iRe-CoDeS framework, briefly introduced in Chapter 2. This bottom-up recovery prediction provides information regarding aggregated recovery demand levels, recovery building states and their spatial and temporal distribution, and finally quantification of resilience metrics. Resilience and recovery quantifications add the dimension of time to building (functionality) loss estimates.

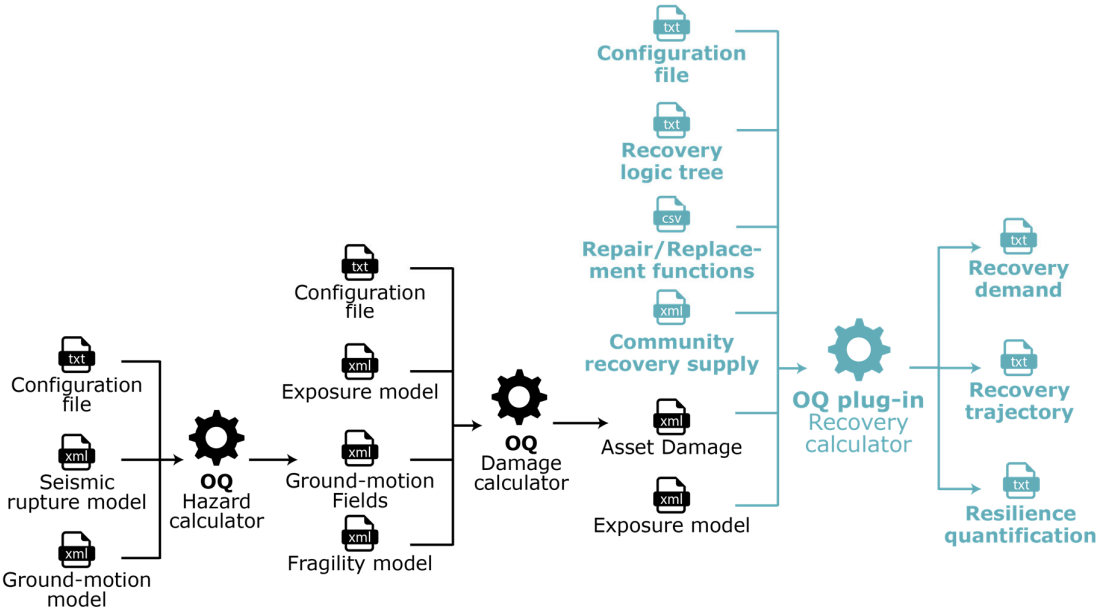


**Figure 2 Inclusion of the recovery plug-in into the OpenQuake calculation flow for a scenario damage evaluation.**

## 3.1 Input files

The plug-in for recovery predictions of an earthquake scenario requires the previously computed earthquake damage scenario. The aggregation of damage-state predictions can be chosen to the level that is required. In addition, an OQ exposure file (in csv-format) is required. Supplemental information on the existing OQ calculators can be found in GEM (2022). Input files, such as exposure model and fragility model, can be found in the European seismic risk model 2020 (ESRM20) published by Crowley, Dabbeek, et al. (2021).

The simulation of RRE trajectories in the OQ-RRE plug-in requires additional information, which needs to be provided in the following input files:

- The ***damage-to-recovery logic tree*** *file* contains the information of the logic tree that transforms damage states of exposure assets, as predicted by the OQ damage calculator, into a sequence of recovery steps that need to be taken to reach a functional state, in this case re-occupancy. Such a logic tree can be composed of simple connections or of probabilistic branches. An example of such a logic tree is provided in Figure 3, where the opacity of the branches shows its respective probability. The logic tree typically contains all the steps that will shape the recovery trajectories, yet a single recovery step may contain additional actions (e.g., the repair action generally also requires previous financing, permitting, and contracting), as shown in Figure 4 for moderately damaged buildings.
- The ***community recovery supply*** *file* describes the availability of recovery resources that characterize the community hit by an earthquake. For each recovery action contained in the damage-to-recovery logic tree the number of operators (e.g., inspectors to perform

inspection actions) and the operation rate (i.e., the number of assets for which an action is performed per day) need to be defined.

- The ***repair/replace functions*** *file* specifies the time required to perform the repair and replacement activities. As evidenced in Tables 1 and 2 of Chapter 2, the repair depends on the initial damage state and therefore, the repair time needs to be defined for each damage state that contains repair actions in the damage-to-recovery logic tree (see Figure 3). In addition, the repair and replacement need may be specified separately for various taxonomies. The current version of the recovery OQ-RRE plug-in is limited to residential buildings, therefore no separation with respect to the building function, as described in HAZUS, is possible.
- The ***configuration file*** contains the information about the path location of the five required input files. In addition, several general definitions of the recovery analysis need to be provided: the duration of the recovery simulation (in days), the number of samples of the logic tree to be performed. The current version of the OQ-RRE plug-in recovery calculator is limited to single-day simulation steps, meaning that recovery is derived after each day following a damaging earthquake, until the specified duration is reached.

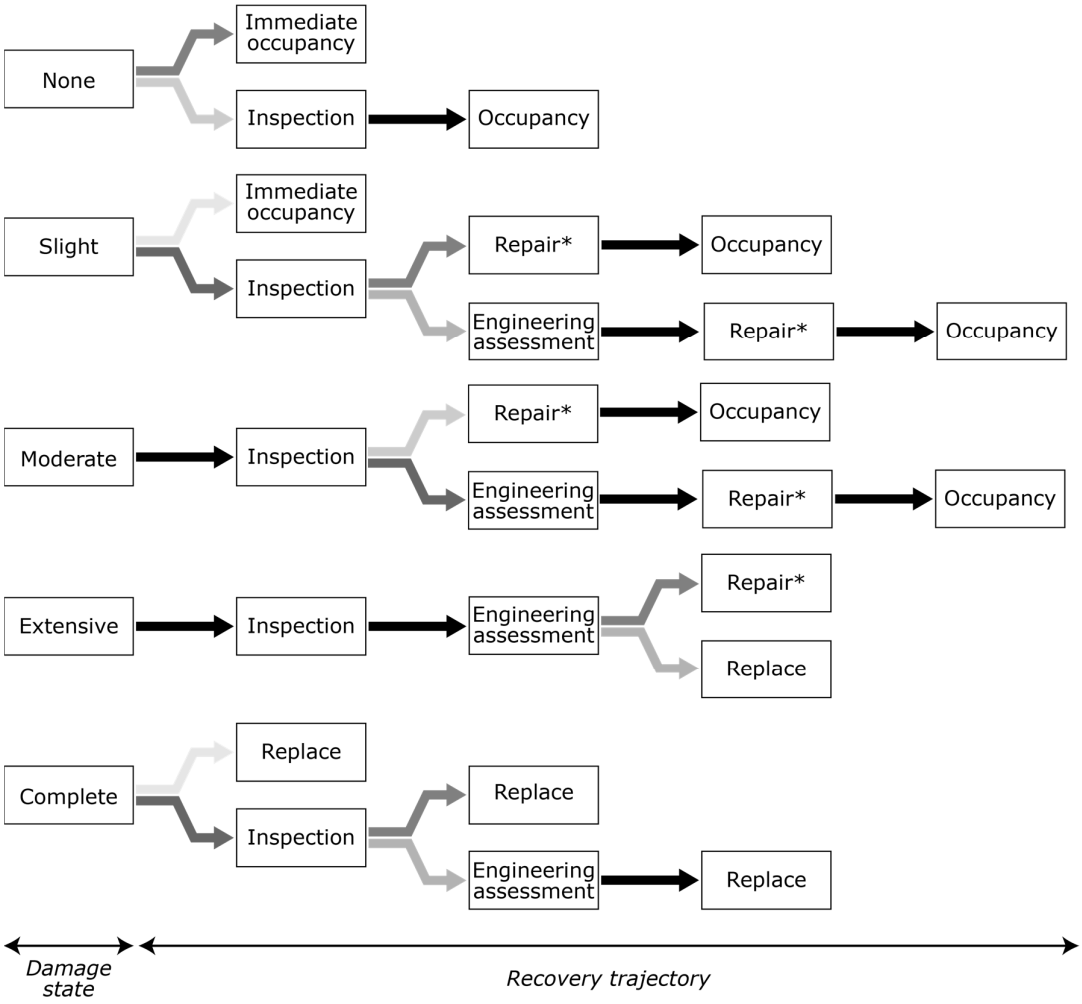


**Figure 3 Example of a damage-to-recovery logic tree. The starting points are HAZUS damage states and the final step considered in this example is re-occupancy. *Repair efforts generally depend on the underlying damage state and may include additional impeding factors, not represented here for better readability of the figure.**

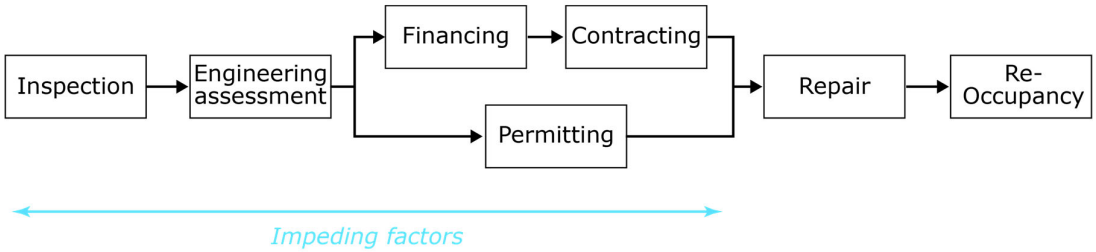


**Figure 4 Example of the sequence of impeding factors preceding repair works for a building in moderate damage state. In the iRe-CoDeS framework, the demand for the previous step needs to be met before demand for the current step is created.**

## 3.2 Output files

In the current version of the OQ-RRE plug-in, three main types of output information are available and can plotted and stored in the following csv-files:

- ***Recovery demand*** is the transformation of damage states to recovery states, providing an overview of the distribution of buildings with respect to the steps that will be required to reach re-occupancy. These steps, which typically include visual inspection, engineering assessment, repair, and replacement of damaged assets, are evaluated on each day following the earthquake and may be useful to detect bottlenecks in the recovery. In the analysis of regional recovery, assets with an open recovery demand are assumed to be unavailable for the level of aimed functionality level (i.e., safe re-occupancy in our case).
- ***Recovery trajectories*** track the recovery progress by exposure asset. Thus, the recovery state of each asset, and the open demand for recovery actions are evaluated every day until the final day of analysis that is specified in the input file. This allows to produce the spatial and temporal evolution of recovery after a damaging earthquake. In addition, the number of buildings that are ready for occupancy or have an expected time of recovery can be tracked.
- ***Resilience quantification*** is obtained by analyzing the recovery trajectories and the evolution of functionality loss over time. Main analysis outcomes are: the lack of resilience (LoR) (Didier et al., 2018), a normalized area enclosed by the function recovery curve; the time to regain a given level of functionality (e.g., 90% of the pre-earthquake level); and the functionality level after a given time period (e.g., the level of functionality 2 months after the earthquake).

  The current version of the OQ-RRE plug-in is intended for residential housing service, which is regained when a building enters the re-occupancy functionality level. The LoR, therefore, returns the un-supplied housing demand, summed of the entire period until recovery of pre-earthquake housing supply is reached. The LoR is, therefore, expressed in units of people-days and is approximated as the number of occupants, specified in the exposure file, for which their home is not available. Thus, the LoR is a crucial indicator, for instance when planning temporary housing.

### 3.3 Calculation workflow

The OQ-RRE plug-in performs, for each time increment, $t_i$, (by default one day) the following calculation steps:

- For each inspection team:
  - Draw a random sample of the inspection rate (number of buildings per day) within the provided bounds.
  - Attribute the inspection team to a randomly selected building.
    - Set the inspection demand to 0. Set the *InspAfter* variable to the current time increment.
    - Based on the damage state of the asset, activate the subsequent demand in the damage-to-recovery tree (by setting it to 1).
  - Until the maximum number of buildings per day is reached, attribute the inspection team to the closes building with an open inspection demand and repeat the previous step.
- For each engineering team:
  - Draw a random sample of the engineering assessment rate within the provided bounds.
  - Attribute the engineering team to a randomly selected building with an open engineering assessment demand.
    - If the maximum number of assessments per day is exceeded (this service may have a rate below 1), reduce the supply of engineering teams for the $(1/EngAssRate) - 1$ following days. Set the *EngAssAfter* variable to $t_i + (1/EngAssRate)$. Set the engineering assessment demand to 0 for the selected building. Based on the damage state of the asset, activate the subsequent demand in the damage-to-recovery tree for the time increment $(1/EngAssRate)$ units after the current time increment (by setting it to 1).
    - If the maximum number of assessments per day is not reached, set the engineering assessment demand to 0 for the selected building. Set the *EngAssAfter* variable to the current time increment. Attribute the engineering team to another random building with an open engineering assessment demand. Based on the damage state of the asset, activate the subsequent demand in the damage-to-recovery tree (by setting it to 1).
- For each team providing repair impeding factors (such as permitting, financing, contracting) follow the same steps than for the engineering teams.
- While not all workers have been attributed:
  - Select an asset with open repair or replacement demand.
  - Randomly attribute the number of workers within the specified bounds.
    - If the selected asset requires repair, divide the repair time by the number of workers.
  - Reduce the supply of workers for the time span [$t_i$, $t_i$+repair/replacement time] by the number of workers.
  - Set the *OccAfter* variable to $t_i$ + repair/replacement time

## 4. Demonstration of the simulator capacities

To verify the OQ-RRE plug-in, demonstrate its capability to predict regional post-earthquake recovery, and analyze its sensitivity to the input parameters, two case studies are presented. First, the canton of Valais (Switzerland), is chosen to present a simulated earthquake and demonstrate the OQ-RRE capabilities in predicting recovery and quantifying resilience with fictitious recovery supply levels. Then, the framework is applied to the real data of the Kraljevo (Serbia) earthquake of 2010, which allows for an indirect validation of the framework. In addition, the Kraljevo case study enables conclusions on the difficulty to estimate important input parameters, such as supply

of resources to resolve the impeding factors, and to assess the influence of rapid damage predictions on the recovery trajectories.

### 4.1 Recovery simulation for a simulated earthquake in the canton of Valais (CH)

The capabilities of the OQ-RRE plug-in recovery calculator are first demonstrated based on a fictitious earthquake scenario in the Swiss canton of Wallis. We use the ground-motion models, site conditions, and exposure database of the ESRM20 model (Crowley, et al., 2021). This exposure database contains the number of buildings, their value, the number of occupants, their taxonomy, and their approximate location (multiple buildings are lumped at the same geo-coordinates).

Based on the exposure model, the canton of Valais comprises a total of 111’033 buildings lumped to 252 building location coordinates. The housing service demand is taken equal to the total number of building occupants, which is the ESRM20 exposure model sums up to 344'145 people. The relative distribution of unreinforced masonry (MUR), reinforced concrete (CR), and other buildings, such as wooden buildings or dual systems, are shown in Figure 5b.

A scenario M5.9 scenario earthquake is simulated, with the epicenter at longitude 7.65 and latitude 46.38; and at a depth of 12km. A summary of the building locations, exposure model and epicentral coordinates is provided in Figure 5a. For the scenario earthquake, the average damage prediction of the ground-motion-field realizations provided by OQ is used. The fragility curves are taken from the ESRM20 model (Romao et al., 2021).

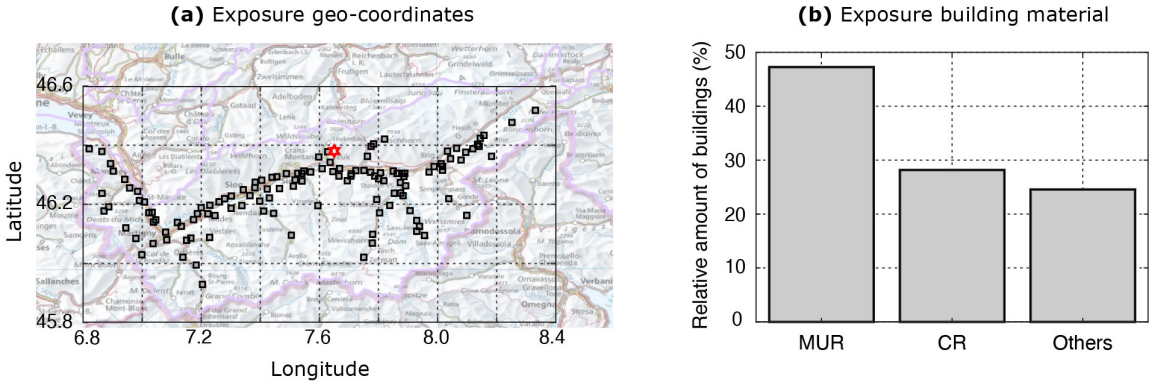


**Figure 5 Geo-coordinates of the building sites with the boundaries of the Valais canton (a) and distribution of relative frequency of encountered building materials (b).**

#### Input for the OQ-RRE plug-in

As described in Section 3.1, the input for the OQ-RRE recovery calculator is comprised of three additional files with respect to the OQ damage scenario calculation. First, the logic tree to link damage states with the sequence of recovery actions is formulated and presented in Table 3. A uniform uncertainty of [-0.1, 0.1] is added to the weights of the logic-tree in the calculator in the simulation. The recovery and replacement functions are estimated based on HAZUS (FEMA, 2004), with some refinements: the repair and replacement time are defined to vary based on the building height and a normal uncertainty is added to the estimated repair times. In addition, ranges to the number of workers that can perform works in parallel are estimated.

The total repair time is divided by the number of workers that work in parallel, while the replacement time is set to the estimated value regardless of the number of workers on site. An overview of the assumed repair and replacement needs for damaged residential buildings is given in Table 4.

The supply of recovery operators is difficult to estimate and depends on many parameters, however, the following values are assumed: 80 inspector teams in the first week and 120 inspectors afterwards; 60 engineering teams in the first 2 weeks and 100 afterwards; 800 workers in the first month, then 1400 until the sixth month, and 1000 afterwards. While the repair and replacement rate of workers is defined in Table 4, the inspection rate is defined to be 7-13 buildings per day and the assessment rate as 0.33 per day. The regional supply of recovery services is based on expert judgement for demonstration purposes and is based on outcomes of the validation case study; hence they may not represent the true preparedness level of the Valais region. The sensitivity of the results to the supply estimation is briefly discussed in Section 4.2.

**Table 3 Weights of the damage-to-recovery logic tree employed in the OQ-RRE plug-in. End nodes, defined as final steps of recovery trajectories, are highlighted in bold.**

| Damage State | First branch | Second branch | Third branch |
|---|---|---|---|
| None | **Re-Occ** (0.75)<br>Insp (0.25) | Re-Occ (1) | |
| Slight | **Re-Occ** (0.15)<br>Insp (0.85) | **Re-Occ** (0.15)<br>**Repair** (0.85) | |
| Moderate | Insp (1) | **Repair** (0.25)<br>EngAss (0.75) | **Repair** (1) |
| Extensive | Insp (1) | EngAss (1) | **Repair** (0.9)<br>**Replace** (0.1) |
| Complete | **Replace** (0.1)<br>Insp (0.9) | EngAss(1) | **Repair** (0.35)<br>**Replace** (0.65) |

**Table 4 Repair and Replacement efforts for residential buildings.**

| Recovery action | Building height | Mean time | St. Dev. time | Number of workers |
|---|---|---|---|---|
| Repair – DS slight | 1 | 3 | 1 | [1,2] |
| | 2 | 4 | 1 | [1,3] |
| | 3+ | 6 | 2 | [2,4] |
| Repair – DS moderate | 1 | 20 | 5 | [1,3] |
| | 2 | 30 | 7 | [2,4] |
| | 3+ | 40 | 9 | [4,6] |
| Repair – DS extensive | 1 | 85 | 25 | [1,4] |
| | 2 | 100 | 25 | [2,5] |
| | 3+ | 115 | 35 | [4,8] |
| Replace | 1 | 120 | 30 | [3,5] |
| | 2 | 130 | 30 | [5,6] |
| | 3+ | 150 | 40 | [5,10] |

### Recovery demand predictions

The first step of the recovery calculator consists in translating damage states to recovery needs. The average predictions are shown in Figure 6. Evidently, most buildings have no damage and thus, most buildings are immediately occupiable. However, it should be noted that the number of immediately re-occupiable buildings depends on the assumption taken for the inspection scheme. While we assume that inspections are mostly on demand, meaning most building owners will not file a request for inspection if there is no visible trace of damage, there may be post-earthquake plans that involve inspection of all buildings in the region with a predicted macro-seismic intensity above a certain threshold.

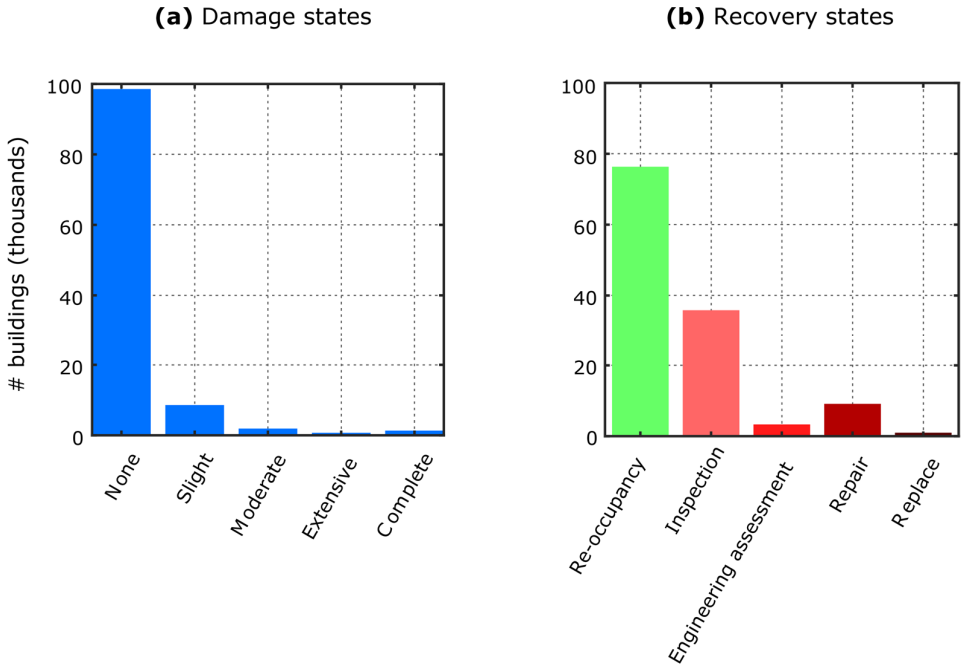


**Figure 6 Predicted average damage states for the scenario M5.9 earthquake (a) and the corresponding recovery services demand (b).**

The iRe-CoDeS framework computes, at each time-step of the recovery process, the demand and supply of recovery services. In Figure 6, the active – or un-supplied – demand for recovery actions are shown for the four main categories: inspection, engineering assessment, repair, and replacement. As the demand for engineering assessment only arises when inspection is accomplished (see Figure 3), the demand for engineering assessment is increasing within the timespan that inspection services are supplied and thus, the inspection demand decreases.

Inspection and assessment rates are much higher than repair and replacement rates, therefore the decrease in buildings with an open demand of repair and replacement works is much slower. Consequently, in the specific case shown in Figure 7, the supply of workers to perform repair and replacement works presents a bottleneck that is hindering rapid recovery. Given the constrained availability of workers and the random attribution to damaged buildings, work supply may be attributed to lengthy replacement activities, while shorter repair actions of slightly damaged buildings have no supply. The iRe-CoDeS framework allows to identify such bottlenecks and may also help in optimal allocation of recovery supply.

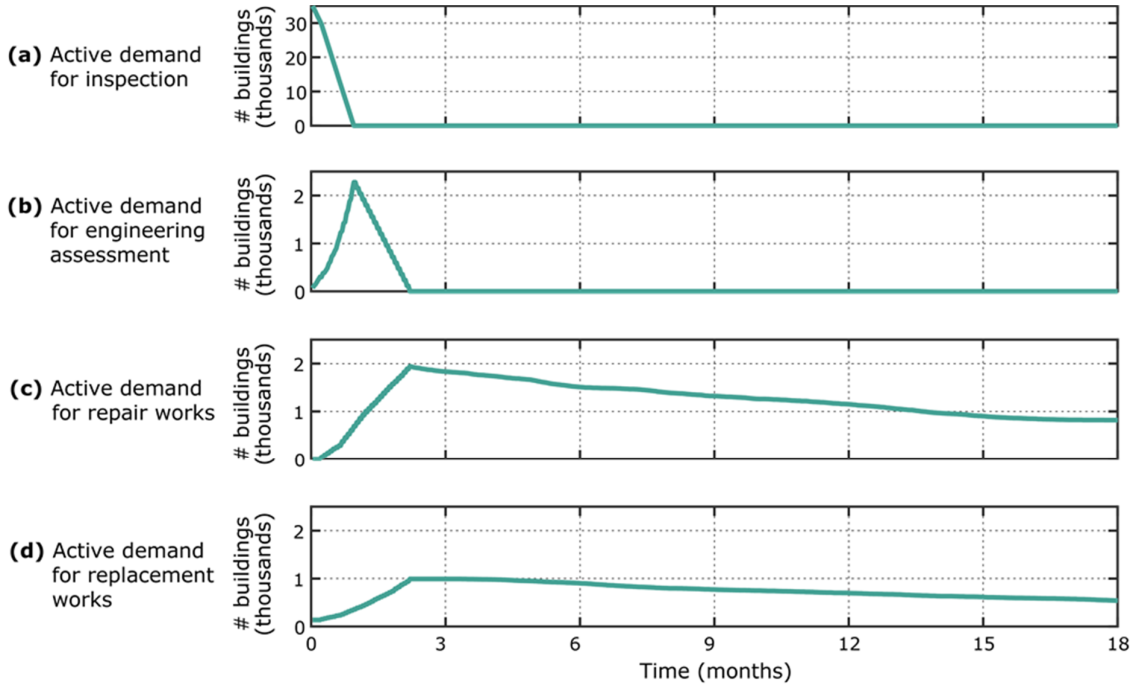


**Figure 7 Evolution of active recovery demand over time. Constrained worker supply and slow repair and replacement rates slow down the rate, at which repair-and-replacement work is supplied.**

## Recovery trajectories

The second set of prediction outputs consists in recovery trajectories. Therefore, the recovery stage of each exposure asset is tracked over time. Aggregating the buildings that reached re-occupancy gives an indication how fast a community is *bouncing back* from the earthquake. Figure 8 shows the evolution of housing supply offered by unreinforced masonry buildings built without seismic design considerations (MUR-CDN) after the simulated M5.9 earthquake scenario. This building category is commonly assumed to be the most vulnerable building type in Switzerland, which is confirmed by the comparison of housing supply recovery of MUR-CDN buildings with all other taxonomies. The increased vulnerability of MUR-CDN buildings is reflected by a deeper drop of housing supply immediately after the earthquake. In addition, the more severe damage sustained by unreinforced masonry buildings require more repair and replacement actions – together with the respective impeding factors – and thus, the housing supply from masonry is lower (in relative terms) than the supply from other taxonomies throughout the 2 years following the earthquake.

As the recovery trajectory is tracked for all assets separately, recovery maps can be created. Figure 9 contains examples of such recovery maps for unreinforced masonry buildings: the immediate loss of housing supply and for three timeframes along the recovery trajectory. As expected, the highest loss of housing supply is observed in vicinity of the epicenter, at longitude 7.65 and latitude 46.38.

In a similar manner, Figure 10, contains a representation of the recovery state of all 7’785 reinforced concrete frame buildings 100 days after the scenario earthquake. For all assets that are not immediately re-occupiable, the achieved day of re-occupancy (in green), the scheduled day of re-occupancy, or the absence of scheduled re-occupancy can be represented.

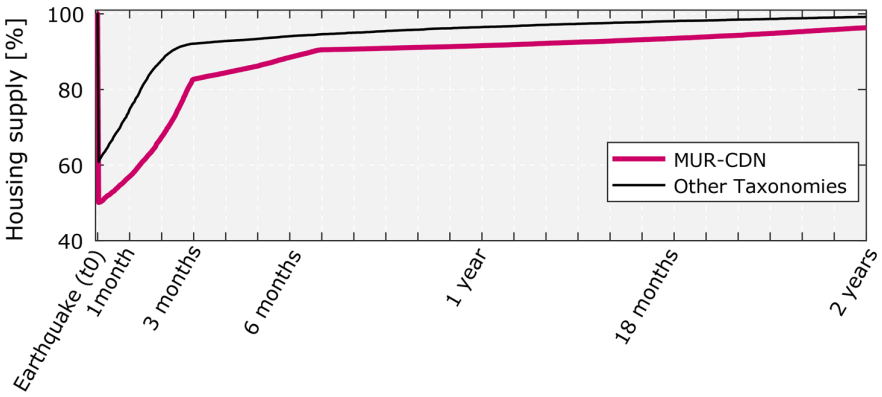


**Figure 8 Evolution of the housing capacity in the canton of Valais after a M5.9 scenario earthquake. The recovery of unreinforced masonry buildings (MUR-CDN) is compared with the other taxonomies.**

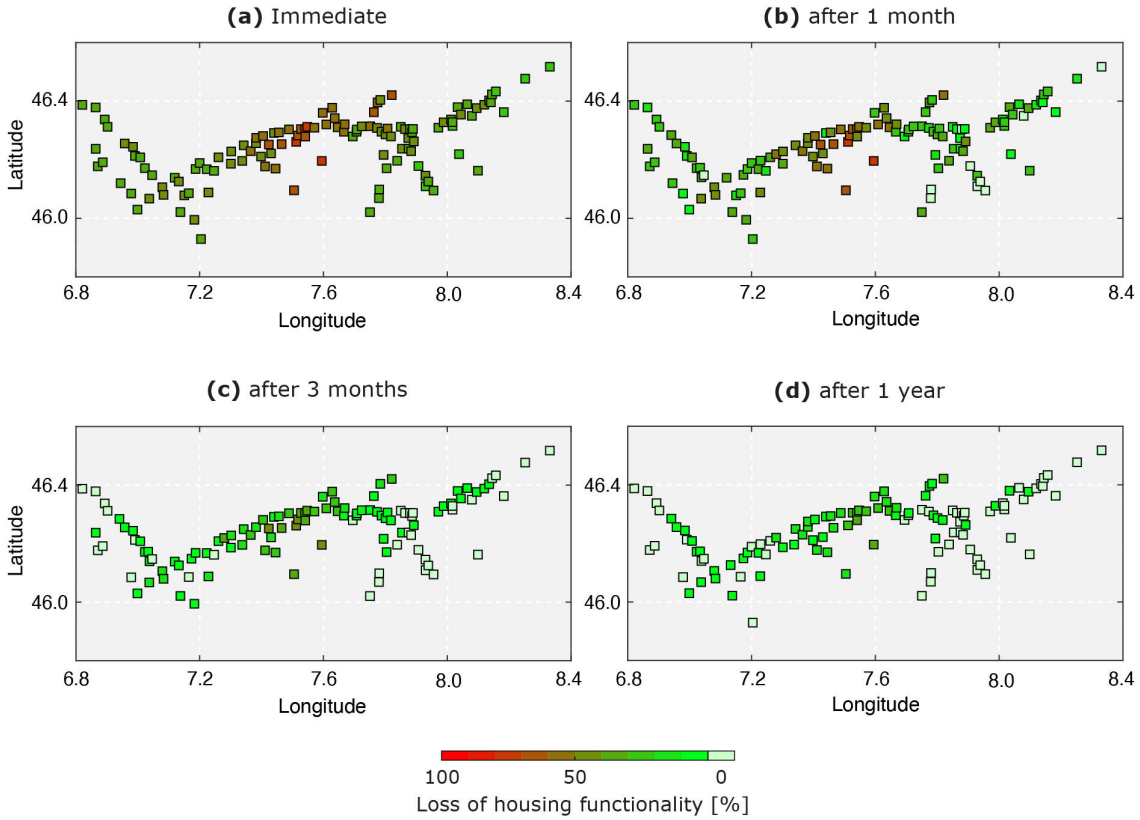


**Figure 9 Recovery trajectory for unreinforced masonry buildings without seismic design (MUR-CDN) after a scenario M5.9 earthquake in the canton of Wallis (Switzerland). Several buildings are lumped into each square and the loss of housing functionality is proportional to the number of buildings being re-occupiable. Geographic location of the squares is presented using degrees of longitude and latitude.**

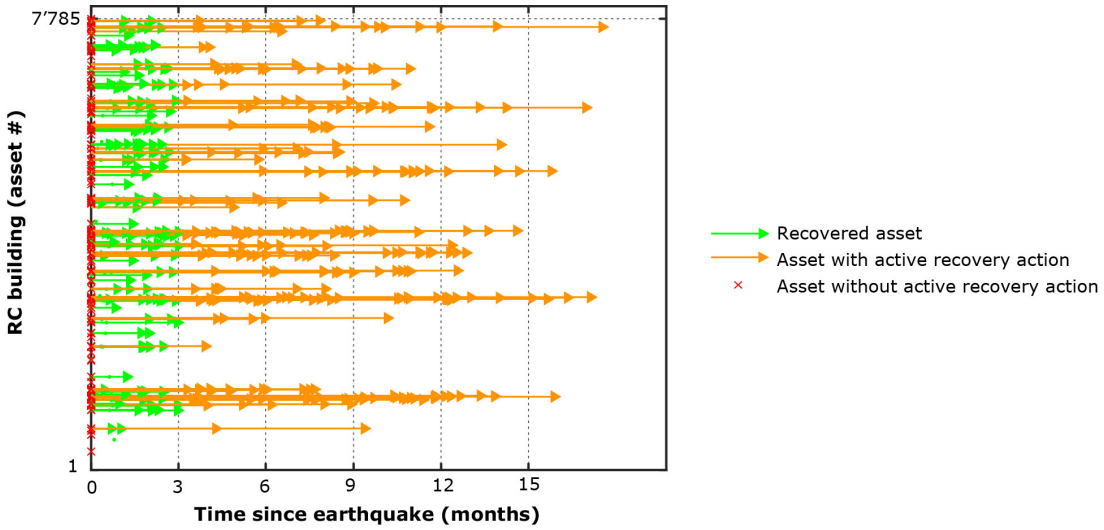


**Figure 10 Evaluation of the recovery state 'by-asset' for RC frames, 100 days after the simulated scenario earthquake. For recovered assets the time after which they became re-occupiable is indicated, for assets with an active recovery action, the scheduled re-occupancy day is indicated, and for assets without active recovery actions the day of re-occupancy is not available yet after 100 days. Assets without any recovery indication did not sustain damage during the earthquake.**

## Resilience quantification

While the recovery trajectories are an important tool to track the state of building assets and the supply demand may prove useful in finding bottlenecks in the recovery supply chain, resilience quantification is crucial for emergency planner and decision-makers. The drop in service supply due to damaged buildings (and infrastructure) and its recovery over time may require mitigation actions. In the case of housing supply, offered by residential buildings, the loss of service supply, shown in Figure 11, may require temporary housing.

The total lack of resilience, in this case over 8 million people-days is a good indicator of the amount of temporary shelter that will be required. In addition, the housing supply level 2 months after the earthquake and the time to regain 90% of pre-earthquake functionality are possible indicators that may help post-earthquake decision-making. The resilience quantification outcomes are reported in Table 5 for the median value and uncertainty ranges (between minimum and maximum) of 20 recovery simulations with fixed supply levels: the uncertainty is generated by random attribution of recovery services and the probabilistic attribution of recovery service demand based on damage-states (see Table 3).

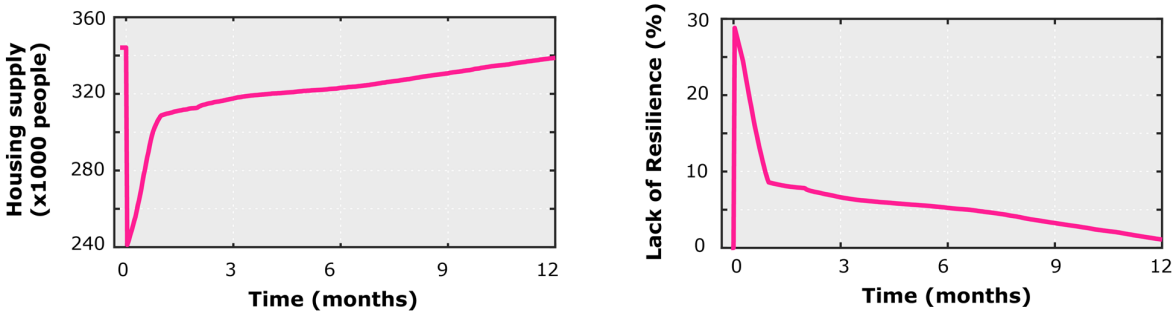


**Figure 11 Drop and recovery of housing supply capacity due to a M5.9 scenario earthquake in Valais (left) and corresponding relative lack of resilience (LoR). Median values of 20 recovery runs are shown.**

**Table 5 Median values of resilience quantification indicators that are provided by the OQ recovery plug-in. Uncertainty bounds from 20 recovery runs with the OQ-RRE plug-in with fixed parameters are provided in brackets.**

| Earthquake scenario | Lack of Resilience | Time to 90% level | Supply level after 2 months |
|---|---|---|---|
| M5.9 Valais | 8'400'000 people-days<br>[8'190'000, 8'526'000] | 35 days<br>[34, 35] | 91%<br>[90%, 92%] |

## 4.2 Relative importance of contributors to RRE

The recovery forecasting with the OQ-RRE depends, in addition to the damage states of buildings, which is predicted with the OpenQuake calculator, on the information contained in the input files described in Section 3.1. While the damage-to-recovery tree and the recovery functions may be derived from heuristics, the supply levels may not always be known.

Therefore, Figure 12 shows the variability in recovery-service demand when increasing or reducing the supply of inspectors, engineers, and workers by 50%. As expected, the number of inspectors influences the entire recovery trajectory, while the number of workers only affects the latter stages: repair and replacement.

In addition, as shown in Figure 13, the number of available inspectors mostly affects the short-term resilience as it governs the slope of the steep initial recovery rate (the elastic recovery, which requires undamaged buildings to be inspected for re-occupancy). On the other hand, the number of workers strongly influences the medium-term recovery, characterized by repair and replacement works. This kind of analysis is important to estimate the sensitivity of predictions to estimated levels of supply, but may also serve recovery-planners to identify good levels of recovery service supply.

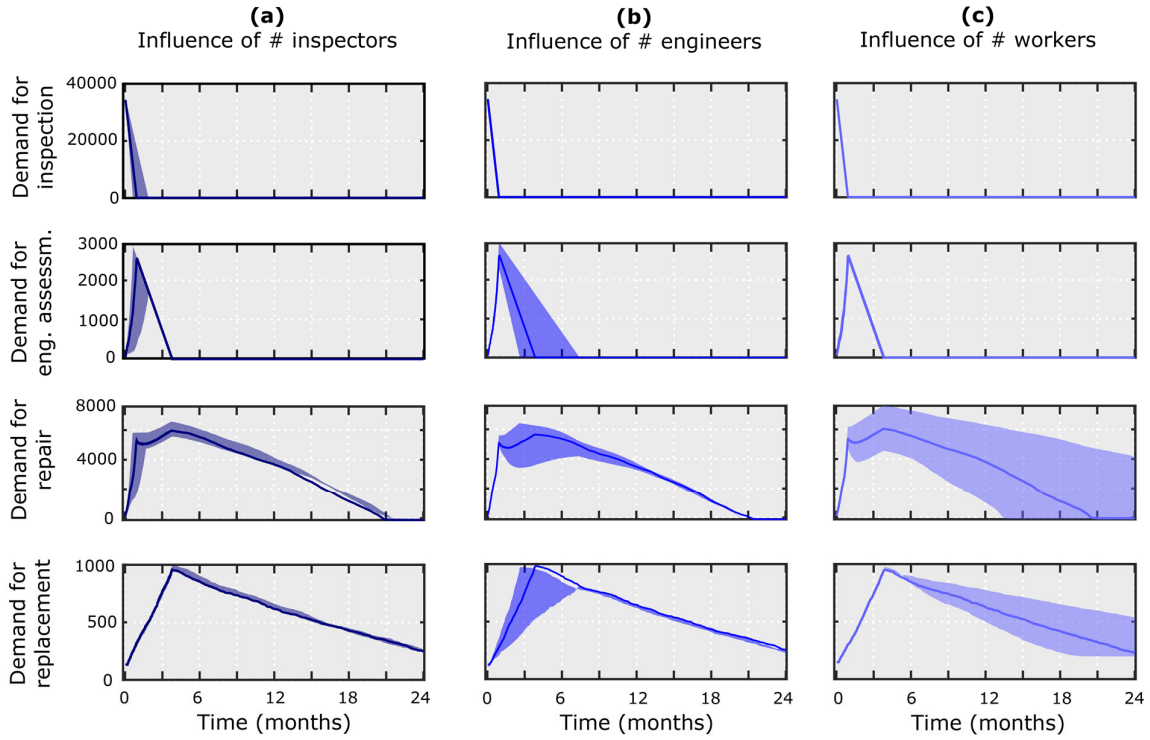


**Figure 12 Uncertainty bound in recovery service demand over time when reducing/increasing the supply of inspectors (a), engineers (b), and workers (c) by 50%. Other impeding factors, such as permitting and contracting are considered as unconstrained in this example.**

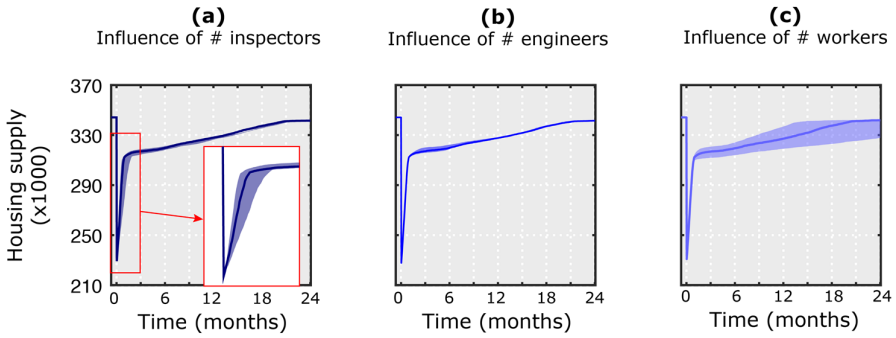


**Figure 13 Uncertainty bound in the evolution of post-earthquake housing supply over time when reducing or increasing the supply of inspectors (a), engineers (b), and workers (c) by 50%.**

The relative sensitivity of predicted resilience-quantification metrics to recovery-service supply levels are compared in Figure 14. The relative sensitivity is calculated as the range of predictions by changing one parameter (in a -50% to +50% range) relative to the median value obtained without changing any parameter. The range of predictions without changing any parameter is indicated as a dotted line in Figure 14 and is related to the random attribution of recovery supply to buildings with an open request.

While the lack of resilience is strongly influenced by the number of workers, the short-term goal of reaching 90% of the pre-earthquake housing supply mostly depends on the number of inspectors. With time passing after the earthquake, the influence of the inspection speed fades and the influence of the supply of workers increases, as can be seen by comparing the relative sensitivity estimates for housing supply after 3 weeks (Figure 14c) and after 3 months (Figure 14,d).

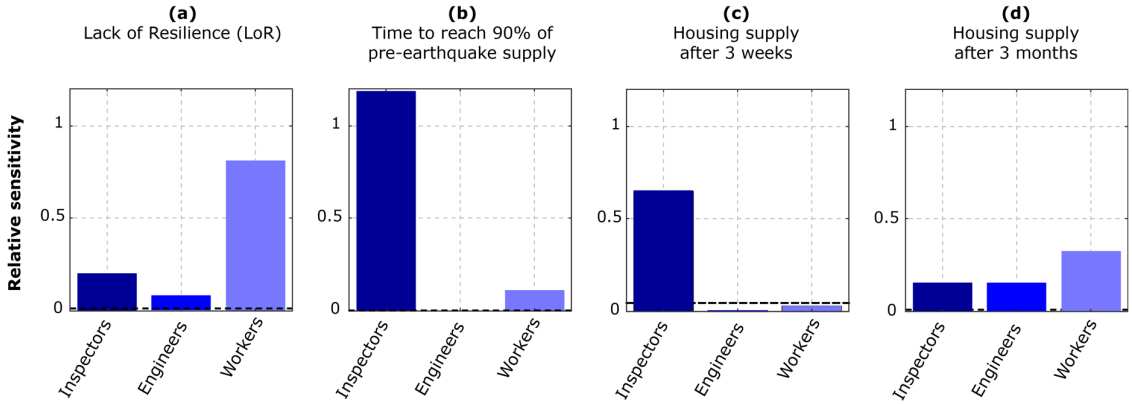


**Figure 14 Relative importance of number of inspectors, engineers, and workers on resilience quantification metrics. The relative sensitivity of resilience quantification metrics with respect to recovery service supply levels is calculated as the ratio between the range of predictions obtained by changing the supply level by +/- 50% and the prediction of the unchanged supply level. The dotted line indicates the uncertainty range from multiple recovery simulations with unchanged recovery service supply.**

### Interdependency of recovery actions and services

As described in Section 2.3, recovery services are not independent. Indeed, the damage-to-recovery logic tree (see Figure 3) tracks the recovery actions that need to be completed before a given recovery action can start and thus, has an open and active demand for the related recovery service. The uncertainty bounds arising from the supply of workers in Figure 12,c are based on unconstrained supply of repair impeding factors, such as financing, permitting, and contracting. Therefore, the influence of a limited supply of permitting services to 60 per day is shown in Figure 15.

In case of constrained permitting, the addition of workers does not reduce the demand for open repair works, which can only be addressed once permitting is completed. The iRe-CoDeS framework allows evaluation of the influence of available recovery services on the recovery trajectory

and thus, may help in studying the influence of institutional decisions, such as accelerated repair permitting and control, on the predicted recovery time and community resilience.

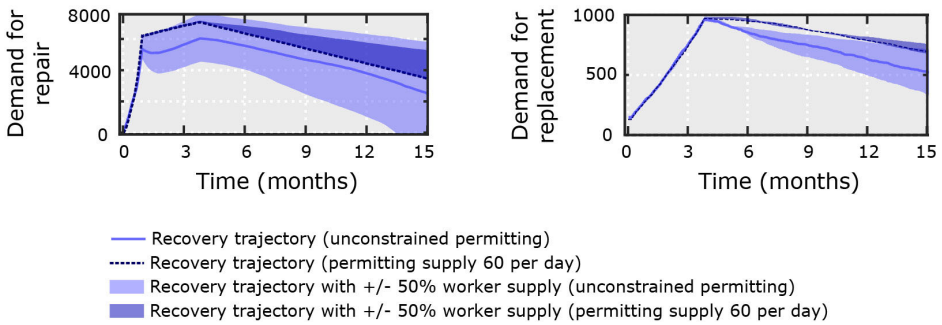


**Figure 15 Influence of constrained supply of permitting services on the uncertainty bounds in recovery service demand over time when reducing/increasing the supply of workers by 50%.**

## 4.3 Recovery setback due to an aftershock

While RRE are performed with the aim to get back to normal, aftershocks or multiple earthquakes within a sequence present possible recovery setbacks. Not only would several buildings require to be re-inspected, thus acting like a reset for recovery, but buildings that are already weakened by the mainshock are also increasingly vulnerable (Iervolino et al., 2020).

In order to showcase the effect of aftershocks, an M5.6 aftershock is simulated in the same region of Valais. The analysis is limited to reinforced-concrete frame buildings without seismic design (CR-LF-CDN), for which state-dependent fragility curves have been developed (Orlacchio et al., 2021). As intensity measure (IM) the geometric mean over 20 spectral acceleration values is chosen, as suggested by (Orlacchio et al., 2021). The geographical distribution of the IM and the number of CR-CDN buildings are provided in Figure 16.

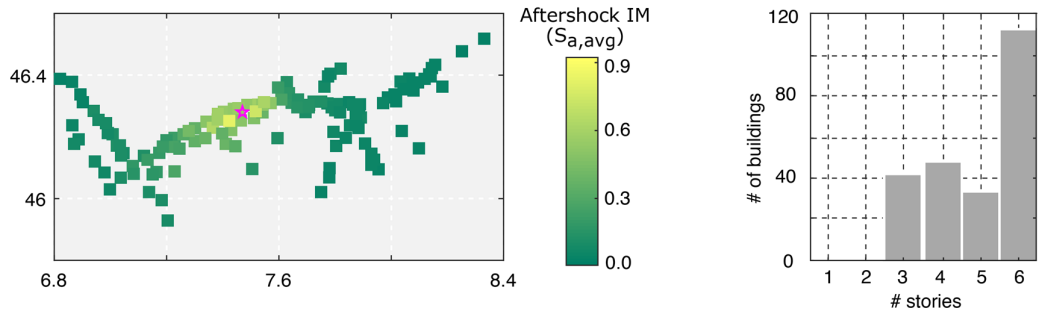


**Figure 16 Median IM map and distribution of building heights of CR-LF-CDN buildings.**

The effect of one aftershock scenario is compared for five building states: (1) the pristine building state corresponds to the assumption that the aftershock would hit intact buildings; (2) the damaged building state corresponds to the aftershock hitting the buildings in their state after the mainshock; (3-5) the damaged building state with partial recovery achieved after 3, 6, and 12 months, respectively. We use the state-dependent fragility functions, based on the Gamma-distribution, proposed by (Orlacchio et al., 2021).

The probabilistic prediction of damage states from the M5.6 aftershock is shown in Figure 17 for the five buildings states. We observe that ignoring the state-dependent fragility produces non-conservative results. The effect of RRE can be observed from the trend towards lower number buildings in the high damage states, as the damage sustained during the mainshock is partially repaired (i.e., for a subset of the buildings, as can be seen in Figure 10). As the more severe damage states, mostly extensive and complete building damage, take longer to get recovered, a

significant reduction in the number of buildings in these damage states after the simulated aftershock is achieved only after 6 months of RRE.

It should be noted that in the current version of the OQ-RRE plug-in recovery calculator, we only consider two building states: either occupiable (repaired) or unavailable (damaged and not repaired yet). The effect of temporary emergency measures to reduce the state-dependent fragility of damaged buildings are not considered.

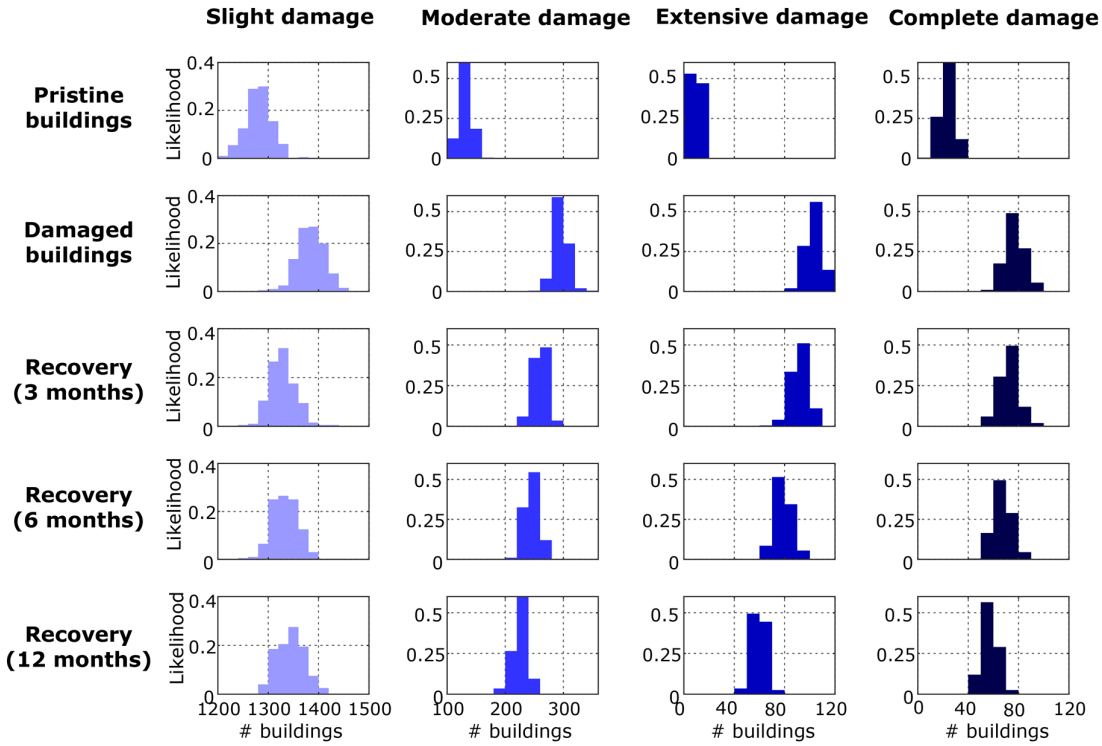


**Figure 17 Building damage states produced by an aftershock. The pristine building state ignores damage accumulation from the main-aftershock sequence, the damaged building state corresponds to damage accumulation, and recovery states account for partial recovery of buildings after 3, 6, and 12 months respectively.**

## 5. Validation based on the 2010 Kraljevo earthquake

As described in Chapters 3 and 4, simulating recovery with a bottom-up methodology, such as the iRe-CoDeS framework implemented in the OQ-RRE plug-in, requires multiple assumptions with respect to demand and supply of recovery actions. While recovery and resilience data from actual earthquakes is still rare, especially in Europe, we use the available information on the Kraljevo 2010 earthquake to attempt a validation of the proposed framework and the developed OQ-RRE plug-in.

Literature sources and personal feedback from local experts, involved in the recovery process, included information regarding the recovery services, which are used to perform recovery predictions in this chapter and thus, this validation case study cannot be considered a *blind prediction*.

### The 2010 Kraljevo earthquake

On November 3, 2010, a 5.4 magnitude earthquake with a focal depth of 13km occurred 4km north of the city of Kraljevo (Serbia) at 1:56AM local time (Seismological Survey of Serbia, 2010). The earthquake caused 2 casualties and 180 injuries.

The damage classification was tailored for the Kraljevo earthquake and contained six damage grades (K1 to K6), ranging from slight damage to collapse. The classification of building damage

was based on six categories: categories K1-K3 did not require major structural repair, as the buildings experienced only minor to major nonstructural damage; damage category K4 and K5 required structural repair, while buildings in category K6 needed replacement. For recovery predictions, K1 and K2 have been merged into 'slight' damage, K3 corresponds to 'moderate' damage, K4 and K5 have been merged to 'extensive' damage, and, finally, K6 corresponds to 'complete' damage. This mapping is based on the simplified four-level damage-classification scheme proposed by (Stojadinovic et al., 2021), yet the damage-state definitions may not exactly match.

## 5.1 Reported repair and recovery efforts

Building inspection started immediately after the earthquake and was carried out by local civil engineers and architects with the goal of establishing life safety (Marinkovic et al., 2018). This process lasted between 10 to 14 days, after which official damage assessment forms were distributed to the inspectors. Subsequent inspections included both: detailed damage inspection with loss estimation as well as building safety assessment. At this stage, surveys were performed by local experts, as well as civil engineers and academics from all Serbian universities (Manic and Bulajic, 2013; Marinkovic et al., 2018).

Local government oversaw the recovery of residential buildings, on which our analysis is focused. Immediate re-occupancy of residential buildings was determined from the assigned damage category: few residential buildings in damage category K5 and all residential buildings in category K6 needed to be immediately evacuated. No multi-family residential buildings, which were mostly built in reinforced concrete, needed evacuation.

The recovery activities that followed the inspection depended on the damage state and the ownership structure (i.e., either single-family or multi-family buildings). Recovery activity sequences were recreated based on interviews with the engineers that oversaw the recovery process for residential buildings and are summarized in Figure 18 (Blagojevic et al., 2022).

The largest portion of residential buildings were recovered 18 months after the disaster. However, delays due to the lack of buildings materials, especially in the immediate period after the earthquake, and due to repair financing postponed building recovery (Marinkovic et al., 2018).

A particularity of the November 3, 2010, Kraljevo RRE lies in the very efficient supply in prefabricated buildings to replace irreparable and collapsed buildings (Marinkovic et al., 2018). In addition, while repair of buildings in damage classes K1 to K3 needed prior financing (from public funding), and repair of buildings in damage classes K4 to K5 required two financing rounds, design, and control of design, the replacement was directly organized by the state-level disaster response. Thus, the replacement time was 15-30 days, significantly less than the repair of multi-family buildings for instance (see Table 6).

Another impeding factor in the case of the Kraljevo recovery, consisted in the meteorological conditions and seasonal workforce. Those irrational delaying factors led to the postponement of repair efforts until spring of 2011 for many repair services. While the OQ-RRE framework offers the capacity to simulate such impeding factors, it has been omitted from the simulation, given the unpredictable nature of this type of delay.

## 5.2 OQ-RRE model input

Repair and recovery needs are estimated based on feedback from experts who were involved in or are familiar with the real RRE after the 2010 Kraljevo earthquake and thus, the damage-to-recovery input file for the OQ-RRE plug-in simulator has been adjusted accordingly, as shown in Figure 18. The iRe-CoDeS framework allows for such a flexible bottom-up modelling of recovery trajectories.

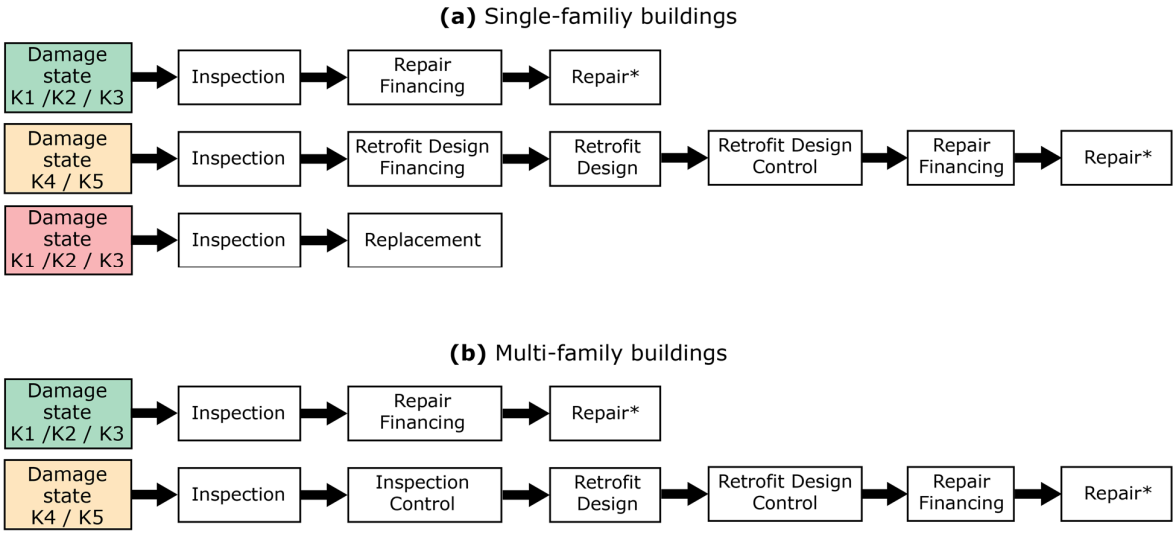


**Figure 18 Damage-to-Recovery logic tree for residential single-family (a) and multi-family buildings (b). Repair times depend on the damage state, as shown in Table 2. In addition, many single-family houses with minor repair (K1-K3) were repaired without professional workers and therefore, a separate worker supply is introduced for this category (see Table 6).**

In addition to the repair functions (Table 2) and the damage-to-recovery logic tree (Figure 18), the supply level of the Kraljevo region needs to be defined. Therefore, publicly available databases are used to collect the necessary information, as shown in Table 6.

**Table 6 Supply capacity for recovery services. Other services are assumed to be unconstrained, given the lack of reliable information.**

| Recovery service | Supply capacity [per day] |
|---|---|
| Inspectors | [50, 100] until day 60, then [10, 20] |
| Engineers | 4 until day 60, then [10, 12] |
| Workers (minor repairs) | [50, 60] until day 120, then [100, 120] |
| Workers (major repairs) | [75, 100] |

## Exposure data

Seismic risk predictions in general and recovery prediction in particular show a large dependency on the quality of the exposure model. Exposure modelling refers to the processes of gathering information from multiple sources and developing tools to estimate building attributes, which are required to perform earthquake risk and consequence predictions but are not directly available in existing databases. An overview of such building attributes and their relevance for classification of buildings is given by (V. Silva et al., 2022). Therefore, refined building-by-building exposure mapping have gained increasing popularity. (Nievas et al., 2022) proposed an exposure model for Cologne (Germany) merging publicly available governmental databases and volunteered graphical information aggregated at various levels of geographical refinement. (Diana et al., 2019) used machine-learning tools to generalize asset taxonomy gathered by visual screening for a subset of buildings in the city of Basel (Switzerland) based on building properties that can be found in public databases.

In a similar manner, we built a bottom-up exposure model for the region of Kraljevo (Blagojevic et al., 2022) to derive building properties that are required for recovery prediction and cannot be found in public databases: the building height, defined by the number of floors; the lateral load-resisting system and material; and the building function. We established and geo-referenced these three attributes for a subset of 1’600 buildings, shown in Figure 19b, through rapid remote visual screening using Google Street view (Anguelov et al., 2010).

For simplicity, based on feedback from local construction professionals, and in order to reduce subjectivity in screening-based attribution of the lateral load-resisting system, only three categories are considered: masonry buildings without lateral confinement; masonry buildings with lateral confinement; and reinforced-concrete buildings.

The exposure modelling starts from an official GIS database, which is provided by the Kraljevo municipality (see Figure 19, left). Hence, for a total of 57'500 buildings in the Kraljevo region, covering all categories and functionalities, the footprint is extracted. In addition, owing to the difference in building height and construction practices between rural and urban neighborhoods, we derived the settlement density as the number of other buildings within a 1km radius, as shown in Figure 20, where the city of Kraljevo can be clearly depicted by the high settlement density.

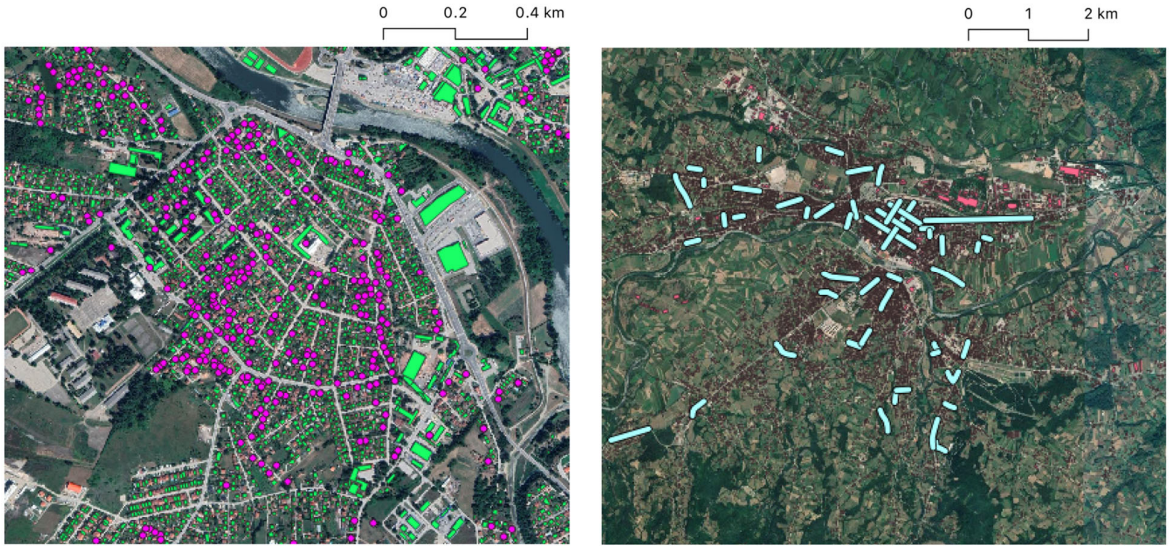


**Figure 19 GIS representation of the Kraljevo census data (green) and the data-set of reported building inspections (purple) on the left; and streets for which rapid screening on Google Street Map has been performed to derive height, function, and lateral load-resisting system.**

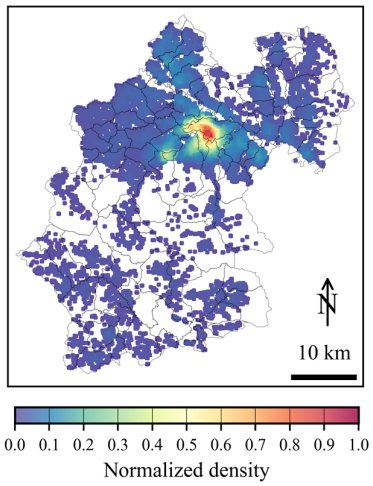


**Figure 20 Normalized settlement density for the Kraljevo region. This derived exposure property is helpful in separating urban from rural areas.**

Multiple, sequential Gaussian-Process (GP) models are used to correlate publicly available building characteristics and the derived properties, such as settlement density, with the three required building properties, as shown in Figure 21. This correlation is trained on the visually labelled dataset of 1'600 buildings (Blagojevic et al., 2022).

The resulting posterior predictive distributions are then used in a conditional prediction workflow to infer missing values. Each GP is composed of a latent function for which the covariance function includes additive correlation terms that measure similarity with respect to the input variables, such as floor area, and a spatial term that assigns higher correlation for spatially close buildings - based on the coordinates.

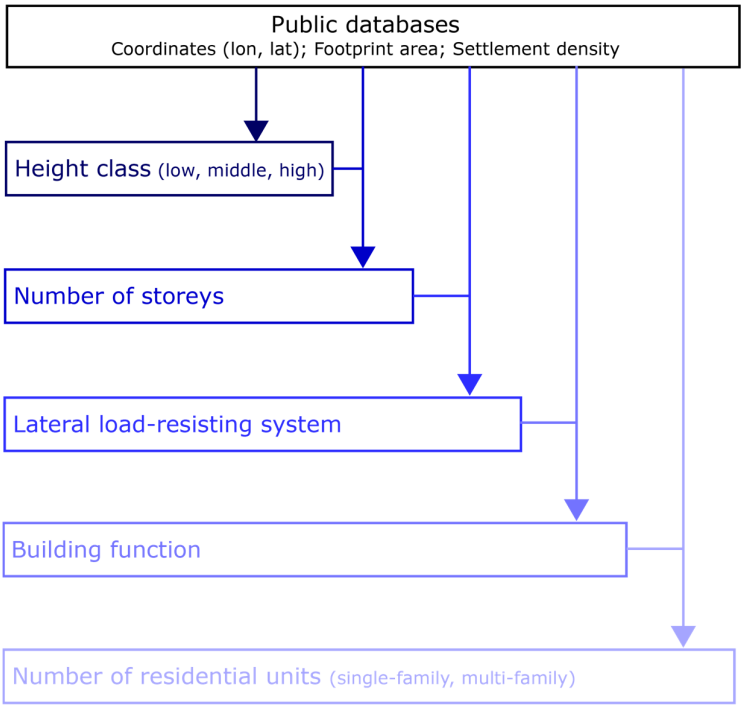


**Figure 21 Sequential Gaussian-Process Models to derive the Kraljevo building-by-building exposure model (Blagojevic et al., 2022). Each arrow corresponds to an individual Gaussian-Process Model, building upon the previous ones.**

The building attributes are assumed to be independent and identically distributed and a posterior is derived. The following ESRM20 fragility functions have been attributed: masonry without lateral confinement is modelled as MUR-LWAL-DNO; masonry with lateral confinement with column-like RC elements is modelled as MCF-LWAL-DUL; and reinforced concrete as CR-LDUAL-DUL.

## 5.3 Comparison of RRE predictions with reported values

For validation purposes, OQ-RRE predictions are compared with available data for 1’193 damaged buildings (Marinkovic et al., 2018). Prediction of the evolution of the recovery of re-occupancy functionality is shown in Figure 22 for buildings predicted to be in the four damage states. Given the evident discrepancy in number of buildings forming the exposure model and number of buildings forming the validation set, the recovery trajectories are provided as relative amount of recovered buildings per damage state (i.e., number of recovered buildings relative to the total amount of buildings in a given damage state).

While direct comparison is difficult, given the limited amount of reported data, the following observations are made in Figure 22:

- In accordance with reports claiming that RRE were mostly accomplished 18 months after the earthquake, 100% buildings are predicted to be recovered after 18 months.
- For buildings in DS1, DS2, and DS4 the predicted end of RREs corresponds to the reported end of the recovery process.
- For all damage states, the reported recovery rate exceeds the predicted recovery rate. While this is mostly attributed to the significantly smaller size of the reported dataset, the delay caused by winter conditions in months 0-6 has not been modelled and therefore, a rather steady increase in recovered assets is observed.

- Buildings requiring replacement had the most straightforward recovery trajectory (see Figure 18), which may explain the fact that recovery of buildings in this state is reproduced with the highest accuracy. Another reason for this observation may be the smaller number of buildings in this state, which makes for a closer match between reported and predicted recovery.

It should be noted that the recovery analysis was limited to residential buildings and thus, interactions or prioritization with recovery of public, commercial, and industrial buildings may be another explanation for discrepancies between reported and predicted recovery trajectories. While the overall prediction capacity is deemed acceptable, additional real-case scenarios will help in improving and validating the predictions.

In addition to the evolution over time of recovered buildings, the evolution of buildings, for which demand for inspection service has been supplied, can be compared between reported and predicted values. The validation of demand and supply of such a recovery impeding factor is an essential step in assessing the choice of a component-level recovery demand/supply model architecture. As can be seen in Figure 23, the comparison between predicted evolution of inspected buildings and two reported validation sources is satisfactory. Thus, the use of the OQ-RRE plug-in to predict the ability of a community that has been hit by an earthquake to bounce back is promising.

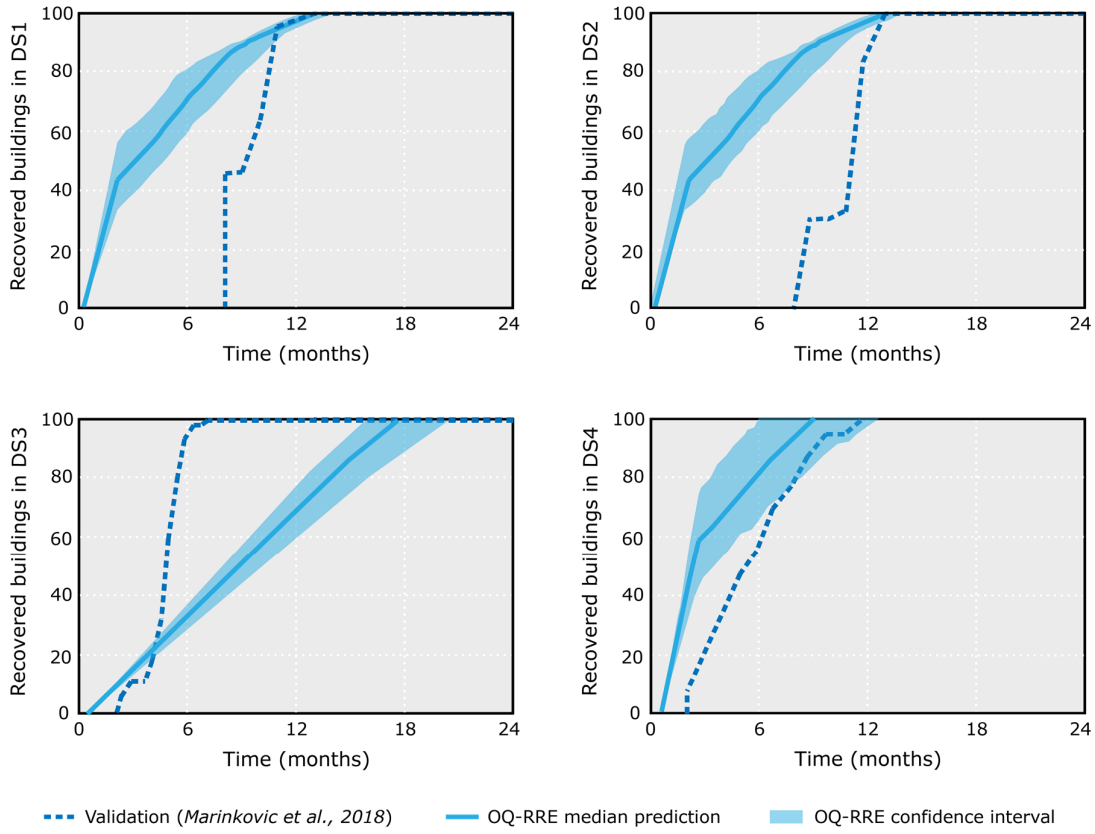


**Figure 22 Recovery predictions for single-family residential buildings after the 2010 Kraljevo earthquake, depending on the initial damage state: DS1 (top left), DS2 (top right), DS3 (bottom left), and DS4 (bottom right).**

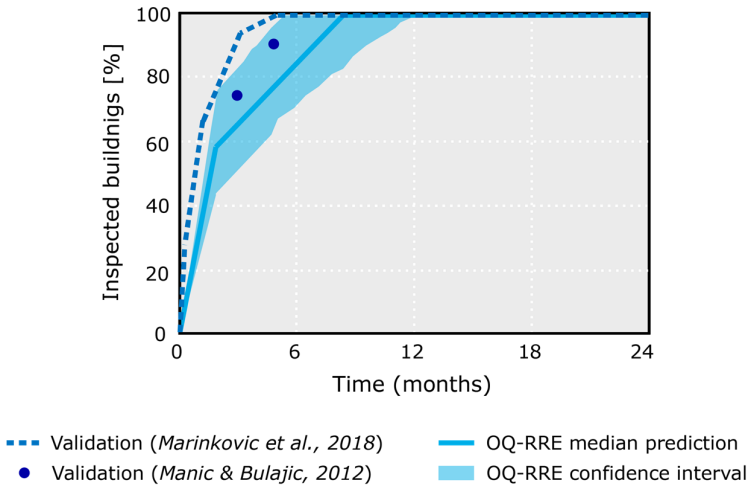


**Figure 23 Validation of predicted time after which inspection service is supplied after the 2010 Kraljevo earthquake.**

## 5.4 Towards dynamically updated risk-model-based recovery predictions

Well-organized recovery efforts may help reducing the duration and the severity of disruptions to important community services such as housing. Yet, the organization of recovery efforts is complicated by intense time pressure and scarce information on the severity and the spatial distribution of earthquake-induced damage. Also, recovery predictions directly depend on the damage prediction or assessment.

Rapid loss-and-damage assessment may be obtained via hazard and vulnerability modules that are potentially combined with recorded ground-motion data from a seismic network. The precision and accuracy of the resulting damage estimates depends, amongst other, on the density of the seismic network, the level of detail of the available exposure information and, finally, how well the fragility functions capture local construction traditions and practices.

While these model-based estimates are particularly helpful in the immediate aftermath, when damage observations are not available yet, the multiple sources of uncertainty motivate the development of a methodological framework to confirm or correct early damage estimates using empirical evidence once available.

Therefore, the DynaRisk project contains a proposal for a machine-learning-based tool that leverages the inspection outcome from the first days following an earthquake to *dynamically* update a regional seismic-risk model and constrain the uncertainties in damage predictions and their geographical distribution (see Figure 24). As the decisions that are taken in the immediate aftermath of an earthquake may shape the entire recovery process, precise information about the damage and its location is a key enabler of increased resilience.

The framework, based on Gaussian-Process (GP) models, not only constrains the damage predictions, but also improves the predicted earthquake intensity measures, exposure mapping, and fragility curves (Bodenmann et al., 2022). Thus, reliable information becomes available in a fraction of the time that would be required to inspect the entire building stock.

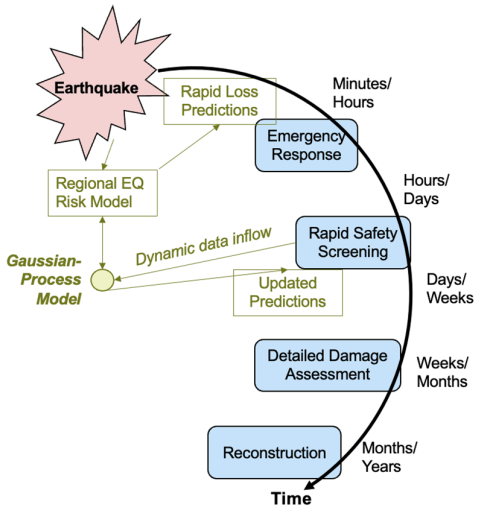


**Figure 24 Use of Gaussian-Process models to infer updated damage predictions by fusing early inspection outcomes with underlying risk-model predictions to reduce the uncertainty of latent functions, such as the ground-motion field.**

## Gaussian-process models

The GP model updates an underlying (latent) function that produces the observations that are used for the updating. In the case of seismic risk, latent functions that may be updated, either separately or simultaneously, are the ShakeMap (Wald et al., 1999), the exposure mapping model, and the fragility functions. The assumptions for updating are briefly exposed in the following, while more detailed information can be found in (Bodenmann et al., 2021a, 2021b).

The modelling of earthquake-induced ground-shaking generally relies on ground-motion models that are derived from recorded intensity measures (IMs) during past events. Conditional on a rupture scenario with characteristics $\boldsymbol{e}$, empirical GMMs are assumed to model the lognormal IM at a site $\boldsymbol{x}$ as

$$\ln(im_i) = m(\boldsymbol{x}_i, \boldsymbol{e}, \boldsymbol{\theta}_m) + \delta_{Wi} + \delta_B,$$

where $m(\cdot)$ denotes the GMM trend function with parameters $\boldsymbol{\theta}_m$ that predicts the median IM based on the magnitude, the style of faulting, the source-to-site distance, and local soil conditions. The within-event ($\delta_{Wi}$) and between-event ($\delta_B$) residuals are independent and both normally distributed with zero mean and variances $\phi^2$ and $\tau^2$, respectively.

The between-event residual, $\delta_B$, models a systematic deviation from the trend function for a given event and therefore is constant for a given event, whereas the remaining variability is summarized in the within-event residual. A simultaneous estimation of IMs at multiple spatially distributed sites, requires assumptions about the dependency structure between their within-event residuals.

Expert-conducted building inspection in the aftermath of an earthquake presents a continuous, yet slow, data inflow that qualifies the induced damage to individual buildings. Recently, Bodenmann et al. have proposed the use of GP models to fuse inspection data with pre-existing exposure, hazard, and vulnerability modules, to dynamically update regional post-earthquake damage estimates. The proposed method leverages observed damage states to reduce the uncertainty of the geographical distribution of the shaking intensity and involves the simultaneous updating of the components governing building damage (Bodenmann et al., 2021a).

### Application to the 2010 Kraljevo earthquake

The comparison between reported and predicted RREs in Section 5.3 relies on the reported damage states of residential buildings. However, as described in Section 5.4, in real-world applications, this knowledge becomes available after months of inspection activities (e.g., after 5 months after the Kraljevo earthquake, as shown in Figure 23). Therefore, we compare, in Figure 25, RRE predictions for buildings having sustained moderate damage:

- Rapid damage assessment based on a predicted shake-map and ESRM20 fragility functions (a),
- dynamically updated damage predictions involving inspection results of 600 buildings, corresponding to approximately 7-10 days of inspection (b),
- the reported number of damaged buildings.

The predicted recovery trajectory for DS2 buildings shows that damage predictions that lack precision and accuracy may undermine good RRE predictions. Thus, the usefulness of tools that fuse observed damage with regional-risk models to dynamically update the predicted damage becomes evident. Future working directions may include the additional updating of RRE functions to reduce the uncertainty in recovery predictions.

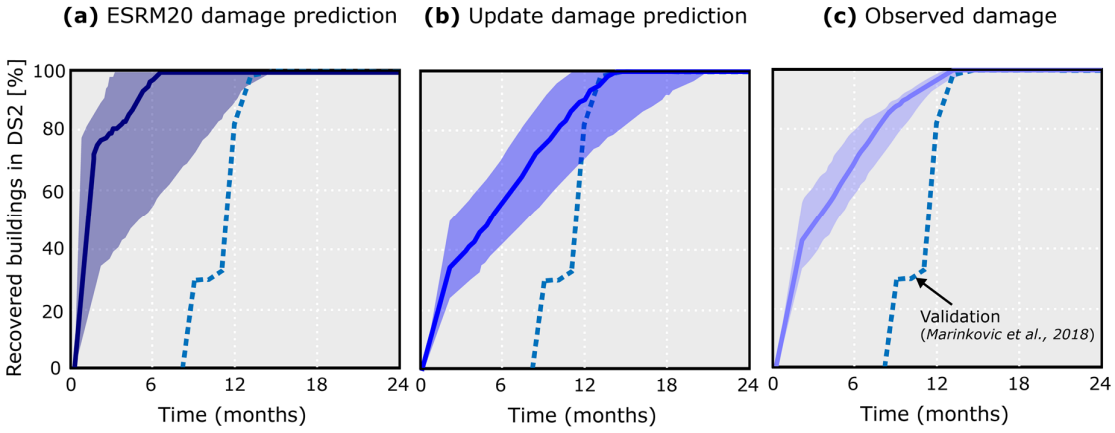


**Figure 25 Dependency of predicted recovery trajectories for buildings in DS2 (moderate damage) on the predicted building damage state. Comparison of recovery predictions based on the ESRM20 damage prediction (a), the ESRM20 prediction after dynamic updating of shake map and fragility curves (b), and the observed damage states (c).**

## 6. Concluding remarks

Within WP4 Task 4.3, a regional forecasting model for post-earthquake repair and recovery efforts has been developed in the form of a plug-in: OQ-RRE. Such a forecasting model is useful to extent loss predictions, from direct losses towards regional lack of supply of services, such as housing, and their duration, leading to a forecast of the lack of resilience. Predicting recovery trajectories at early stages after an earthquake and quantifying the resilience – and the lack thereof – is an important tool for recovery planners. In addition, tracking the progress of recovery is important to predict the time-varying seismic risk of communities that have been hit by an earthquake.

The capacity of the OQ-RRE plug-in to extend the OpenQuake earthquake scenario damage engine towards RRE simulation based on the iRe-CoDeS compositional supply and demand resilience quantification framework has been demonstrated and typical input and output files have been described.

This developed OQ-RRE plug-in and the recovery forecast it provides were verified and validated using the 2010 Kraljevo post-earthquake recovery data, showing acceptable agreement with reported recovery durations.

## 6.1 Discussion and outlook on future working directions

Bottom-up models for community resilience modelling and simulation, such as the iRe-CoDeS framework, present recovery analysts with useful tools to identify bottlenecks in recovery. However, as shown in the validation example presented in Chapter 5, large amounts of data are needed, while simultaneously many assumptions are made to facilitate the analysis, for which the actual values may not be known in the immediate aftermath of an earthquake. While Section 5.4 contains a proposal to reduce the uncertainty in the risk analysis components, the recovery service supply requires some assumptions in absence of precise knowledge. Future efforts are required to establish reliable estimates of these supply levels, as well as of the exact damage-to-recovery transformation. The framework for fusing observed and predicted data, presented in Section 5.4, may be generalized in order to enable updating of the recovery trajectories and the underlying function with early recovery data.

Feedback from risk modelers and recovery practitioners will allow to improve the recovery model. Rigorous data collection on recovery after earthquakes will allow to calibrate models and to get more realistic estimates for the supply of recovery actions. In addition, socio-economic indicators, such as the penetration and level of insurance, levels of private savings, and the economic tissue influence the level of preparedness of a community and thus their resilience and ability to bounce back (Burton & Silva, 2019; World Bank Group, 2020).

While the application in this report is limited to post-earthquake early recovery predictions, the developed OQ-RRE plug-in may be combined with classical risk analysis to improve ex-ante preparedness levels and thus, to improve resilience. In addition, recovery service supply levels that are required to achieve pre-defined performance targets may be derived with this kind of analysis.

Another possible improvement of the recovery prediction is linked to additional functionality states, such as stability, shelter-in-place, functional recovery, and full recovery. These additional recovery states allow to track the advancement of recovery more precisely as buildings move from one recovery state to the next and thus, may provide more refined estimates of time-varying seismic risk. However, as some of these recovery states involve service networks, such as electricity, telecommunication, and water, which are interdependent, precise knowledge of their fragility and geographical position, as well as redundancy in the networks, would need to be known. While the recovery of these networks may be challenging to predict, the building RRE are not independent from these network systems either, as water, power, and, above all, transportation services need to be supplied for repair work to start. In addition, recovery can be seen as a social process that requires decision-making at many levels and thus, involves social and institutional capacities as well (Burton et al., 2022).

Regional repair cost estimates are provided in WP4 task 4.1. Such estimates, for structural and non-structural elements, are typically provided as percentage of building replacement cost conditional on the building damage state. In addition, sources like HAZUS provide median values and thus, neglect the large uncertainties pertaining to repair costs (C. Molina et al., 2022). A probabilistic assessment of repair cost and their specification for intermediate functionality levels presents potential future work and would allow for the assessment of repair cost over time.

The influence of recovery on the state-dependent fragility, for instance during aftershocks, has been shortly described in Section 4.3. However, a more realistic representation of this scenario would require including temporary emergency measures to safeguard buildings in the aftermath of an earthquake, as repair activities that aim at bringing the building back to pre-earthquake levels of physical fragility may not be the optimal choice, when faced with the risk of aftershocks. Additional recovery states would enable more detailed decision-making with respect to time-varying seismic risk.

The uncertainty reduction achieved with the Gaussian-process model in Section 5.3 provides results that are aggregated at the level of a district or a zip-code. The application at building level is not recommended, as it may lead to erroneous conclusions for specific buildings. Consequently, this tool is helpful in reducing uncertainty and giving decision-makers reliable information when planning recovery and estimating required level of recovery supplies. Yet, no active improvement in resilience, through a reduction in inspection demand is achieved. Combining the framework with structural-health-monitoring data may help actively improving short-term resilience of communities facing earthquake risk.

### 6.2 Conclusions

Predicting the recovery of a community hit by a damaging earthquake and the corresponding loss of functionality (or structural downtime) is among the most challenging consequence predictions. A bottom-up simulation tool has been developed to extend the scenario damage calculator capacities of the OpenQuake with building-by-building recovery and resilience predictions. The recovery calculator is implemented as a plug-in, called OQ-RRE, which can be run after damage scenario prediction. The conclusions of demonstrating and validating the iRe-CoDeS framework are as follows:

- The recovery OQ-RRE plug-in has been successfully implemented and provides an overview of recovery service demand, recovery trajectories, recovery maps, and resilience quantification. These parameters provide a crucial overview of the capacity of a community to bounce back after a damaging earthquake.
- While it is difficult to predict how exactly a community reacts to a damaging earthquake and the current framework does not include many important parameters such as socio-economic parameters, such a framework can help in identifying bottlenecks and compare several post-earthquake response measures.
- Comparison with real data characterizing the recovery after the 2010 Kraljevo earthquake shows that the framework produces realistic outcomes. Yet, some irrational and unpredictable recovery delays, like seasonal weather and workforce, cannot be modelled without knowledge that has been gathered after recovery.
- The proposed OQ-RRE plug-in provides flexibility with respect to recovery decisions and institutional decisions.

## 7. References

Alisjahbana, I., Eeri, M., Kiremidjian, A., & Blume, J. A. (2020). Modeling housing recovery after the 2018 Lombok earthquakes using a stochastic queuing model: *Earthquake Spectra*, *37*(2), 587–611. https://doi.org/10.1177/8755293020970972

Almufti, I., & Willford, M. (2013). *REDi Rating System*.

Anguelov, D., Dulong, C., Filip, D., Frueh, C., Lafon, S., Lyon, R., Ogale, A., Vincent, L., & Weaver, J. (2010). Google Street View: Capturing the World at Street Level. *Computer*, *43*(6), 32–38. https://doi.org/10.1109/MC.2010.170

Blagojevic, N., Bodenmann, L., Reuland, Y., & Stojadinovic, B. (2022). The case of 2010 Kraljevo earthquake: Validating a regional recovery model and investigating measures to increase disaster preparedness. *ASCE Natural Hazards Review*, *submitted*.

Blagojevic, N., Didier, M., & Stojadinovic, B. (2021a). *Quantifying Component Importance for Disaster Resilience of Communities with Interdependent Civil Infrastructure Systems*. https://engrxiv.org/hzmy8/

Blagojevic, N., Didier, M., & Stojadinovic, B. (2021b, December 14). Simulating the role of transportation infrastructure for community disaster recovery. *Proceedings of the Institution of Civil Engineers - Bridge Engineering*. https://doi.org/10.1680/JBREN.21.00018

Blagojevic, N., Hefti, F., Henken, J., Didier, M., & Stojadinovic, B. (2021). Quantifying Disaster Resilience of Communities with Interdependent Civil Infrastructure Systems. *EngrXiv*.

Blagojević, P., Brzev, S., & Cvetković, R. (2021). Simplified Seismic Assessment of Unreinforced Masonry Residential Buildings in the Balkans: The Case of Serbia. *Buildings 2021, Vol. 11, Page 392*, *11*(9), 392. https://doi.org/10.3390/BUILDINGS11090392

Bodenmann, L., Reuland, Y., & Stojadinovic, B. (2021a). Dynamic Updating of Building Loss Predictions Using Regional Risk Models and Conventional Post-Earthquake Data Sources. *Proceedings of the 31st European Safety and Reliability Conference*. https://doi.org/10.3929/ethz-b-000507866

Bodenmann, L., Reuland, Y., & Stojadinovic, B. (2021b). Using regional earthquake risk models as priors to dynamically assess the impact on residential buildings after an event. *Published Papers of 1st Croatian Conference on Earthquake Engineering, 1CroCEE, Zagreb, Croatia, March 22nd to 24nd, 2021*, 71. https://doi.org/10.5592/CO/1CROCEE.2021.71

Bodenmann, L., Reuland, Y., & Stojadinovic, B. (2022). sing Gaussian Process Models for Dynamic Post-Earthquake Impact Estimation with Regional Risk Predictors. *Bulletin of Earthquake Engineering*, *submitted*.

Böse, M., Papadopoulos, A. N., Danciu, L., Clinton, J. F., & Wiemer, S. (2022). Loss-Based Performance Assessment and Seismic Network Optimization for Earthquake Early Warning. *Bulletin of the Seismological Society of America*. https://doi.org/10.1785/0120210298

Bruneau, M., Chang, S. E., Eguchi, R. T., Lee, G. C., O'Rourke, T. D., Reinhorn, A. M., Shinozuka, M., Tierney, K., Wallace, W. A., & von Winterfeldt, D. (2003). A Framework to Quantitatively Assess and Enhance the Seismic Resilience of Communities. *Earthquake Spectra*, *19*(4), 733–752. https://doi.org/10.1193/1.1623497

Burton, C. G., & Silva, V. (2019). Assessing Integrated Earthquake Risk in OpenQuake with an Application to Mainland Portugal: *Earthquake Spectra*, *32*(3), 1383–1403. https://doi.org/10.1193/120814EQS209M

Burton, C. G., Toquica, M., Asad, K. M. bin, & Musori, M. (2022). Validation and development of composite indices for measuring vulnerability to earthquakes using a socio-economic perspective. *Natural Hazards*. https://doi.org/10.1007/s11069-021-05095-9

Burton, H. v, Deierlein, G., Lallemant, D., & Lin, T. (2015). Framework for Incorporating Probabilistic Building Performance in the Assessment of Community Seismic Resilience. *Journal of Structural Engineering*, *142*(8), C4015007. https://doi.org/10.1061/(ASCE)ST.1943-541X.0001321

Burton, H. v., Miles, S. B., & Kang, H. (2019). Integrating Performance-Based Engineering and Urban Simulation to Model Post-Earthquake Housing Recovery: *Earthquake Spectra*, *34*(4), 1763–1785. https://doi.org/10.1193/041017EQS067M

Cornell, C. A., & Krawinkler, H. (2000). *Progress and challenges in seismic performance assessment*. PEER Center News, 3(2), Https://Apps.Peer.Berkeley.Edu/News/2000spring/Index.Html.

Costa, R., Haukaas, T., & Chang, S. E. (2020). Agent-based model for post-earthquake housing recovery: *Https://Doi.Org/10.1177/8755293020944175*, *37*(1), 46–72. https://doi.org/10.1177/8755293020944175

Cremen, G., Seville, E., & Baker, J. W. (2020). Modeling post-earthquake business recovery time: An analytical framework. *International Journal of Disaster Risk Reduction*, *42*, 101328. https://doi.org/10.1016/J.IJDRR.2019.101328

Crowley, H., Dabbeek, J., Despotaki, V., Rodrigues, D., Martins, L., Silva, V., Romao, X., Pereira, N., Weatherill, G., & Danciu, L. (2021). *European Seismic Risk Model (ESRM20)*.

Crowley, H., Despotaki, V., Silva, V., Dabbeek, J., Romão, X., Pereira, N., Castro, J. M., Daniell, J., Veliu, E., Bilgin, H., Adam, C., Deyanova, M., Ademović, N., Atalic, J., Riga, E., Karatzetzou, A., Bessason, B., Shendova, V., Tiganescu, A., … Hancilar, U. (2021). Model of seismic design lateral force levels for the existing reinforced concrete European building stock. *Bulletin of Earthquake Engineering*, *19*(7), 2839–2865. https://doi.org/10.1007/S10518-021-01083-3/FIGURES/6

de Iuliis, M., Kammouh, O., Cimellaro, G. P., & Tesfamariam, S. (2019). Resilience of the Built Environment: A Methodology to Estimate the Downtime of Building Structures Using Fuzzy Logic. *Resilient Structures and Infrastructure*, 47–76. https://doi.org/10.1007/978-981-13-7446-3_2

del Vecchio, C., di Ludovico, M., Pampanin, S., & Prota, A. (2018). Repair Costs of Existing RC Buildings Damaged by the L'Aquila Earthquake and Comparison with FEMA P-58 Predictions. *Earthquake Spectra*, *34*(1), 237–263. https://doi.org/10.1193/122916EQS257M

Diana, L., Thiriot, J., Reuland, Y., & Lestuzzi, P. (2019). Application of association rules to determine building typological classes for seismic damage predictions at regional scale: The case study of basel. *Frontiers in Built Environment*, *5*, 51. https://doi.org/10.3389/FBUIL.2019.00051/BIBTEX

Didier, M., Abbiati, G., Hefti, F., Broccardo, M., & Stojadinovic, B. (2018, February). Damage Quantification in Plastered Unreinforced Masonty Walls using Digital Image Correlation. *Proceedings of the 10th Australian Masonry Conference (10AMC)*.

Didier, M., Broccardo, M., Esposito, S., & Stojadinovic, B. (2018). A compositional demand/supply framework to quantify the resilience of civil infrastructure systems (ReCoDeS). *Sustainable and Resilient Infrastructure*, *3*(2), 86–102. https://doi.org/10.1080/23789689.2017.1364560

EERI. (2016). EERI Policy White Paper Creating Earthquake-Resilient Communities. *Earthquake Engineering Research Institute*. www.eeri.org

FEMA. (2004). *HAZUS-MH Technical Manual*. Federal Emergency Management Agency.

FEMA. (2018). *Seismic Performance Assessment of Buildings FEMA P-58-1 Methodology*.

FEMA. (2019). *Seismic Performance Assessment of Buildings FEMA P-58-2 Implementation guide*. Applied Technology Council.

GEM. (2022). *The OpenQuake-engine User Manual. Global Earthquake Model (GEM) OpenQuake Manual for Engine version 3.13.0.*

Iervolino, I., Chioccarelli, E., & Suzuki, A. (2020). Seismic damage accumulation in multiple mainshock–aftershock sequences. *Earthquake Engineering & Structural Dynamics*, *49*(10), 1007–1027. https://doi.org/10.1002/EQE.3275

Kappos, A., Lekidis, V., Panagopoulos, G., Sous, I., Theodulidis, N., Karakostas, C., Anastasiadis, T., Salonikios, T., & Margaris, B. (2007). Analytical Estimation of Economic Loss for Buildings in the Area Struck by the 1999 Athens Earthquake and Comparison with Statistical Repair Costs. *Earthquake Spectra*, *23*(2), 333–355. https://doi.org/10.1193/1.2720366

Karbassi, A., & Lestuzzi, P. (2014). *Seismic risk for existing buildings in Switzerland – development of fragility curves for masonry buildings*.

Marinkovic, D., Stojadinovic, Z., Kovacevic, M., & Stojadinovic, B. (2018). 2010 Kraljevo Earthquake Recovery Process Metrics Derived from Recorded Reconstruction Data. *16th European Conference on Earthquake Engineering*.

Marinkovic, D., Stojadinovic, Z., Kovacevic, M., & Stojadinovic, B. (2019). 2010 Kraljevo earthquake recovery process metric derived from recorded reconsruction data. *16th European Conference on Earthquake Engineering*.

Martins, L., & Silva, V. (2021). Development of a fragility and vulnerability model for global seismic risk analyses. *Bulletin of Earthquake Engineering*, *19*(15), 6719–6745. https://doi.org/10.1007/S10518-020-00885-1

Mieler, M., Paul, N., Almufti, I., & Lee, J. (2018). Predicting earthquake-induced downtime in buildings: An overview of the state of the art . *Proceedings of the 11th National Conference in Earthquake Engineering*. https://www.researchgate.net/publication/326304859

Mieler, M. W., Asce, A. M., & Mitrani-Reiser, J. (2017). Review of the State of the Art in Assessing Earthquake-Induced Loss of Functionality in Buildings. *Journal of Structural Engineering*, *144*(3), 04017218. https://doi.org/10.1061/(ASCE)ST.1943-541X.0001959

Moehle, J., & Deierlein, G. G. (2004). A framework methodology for performance-based earthquake engineering. *13th World Conference on Earthquake Engineering*. https://www.researchgate.net/publication/228706335

Molina, C., Eeri, H. M., Vahanvaty, T., Eeri, M., Kourehpaz, P., & Hutt, C. M. (2022). An analytical framework to assess earthquake-induced downtime and model recovery of buildings: *Earthquake Spectra*. https://doi.org/10.1177/87552930211060856

Molina, S., Lang, D. H., & Lindholm, C. D. (2010). SELENA – An open-source tool for seismic risk and loss assessment using a logic tree computation procedure. *Computers & Geosciences*, *36*(3), 257–269. https://doi.org/10.1016/J.CAGEO.2009.07.006

Nievas, C. I., Pilz, M., Prehn, K., Schorlemmer, D., Weatherill, G., & Cotton, F. (2022). Calculating earthquake damage building by building: the case of the city of Cologne, Germany. *Bulletin of Earthquake Engineering*, *20*(3), 1519–1565. https://doi.org/10.1007/S10518-021-01303-W/FIGURES/21

Orlacchio, M., Chioccarelli, E., Baltzopoulos, G., & Iervolino, I. (2021). State-dependent seismic fragility functions for Italian reinforced concrete structures: preliminary results. *31st European Safety and Reliability Conference - ESREL 2021*.

Potter, S. H., Becker, J. S., Johnston, D. M., & Rossiter, K. P. (2015). An overview of the impacts of the 2010-2011 Canterbury earthquakes. *International Journal of Disaster Risk Reduction*, *14*, 6–14. https://doi.org/10.1016/J.IJDRR.2015.01.014

Reuland, Y. ;, Martakis, P. ;, & Chatzi, E. (2021). Damage-sensitive features for rapid damage assessment in a seismic context. In A. Cunha & E. Caetano (Eds.), *Proceedings of the International Conference on Structural Health Monitoring of Intelligent Infrastructure* (pp. 613–619). International Society for Structural Health Monitoring of Intelligent Infrastructure (ISHMII). https://doi.org/10.5281/ZENODO.5542288

Romao, X., Pereir, J. M., Castro, H., Crowley, H., Silva, V., Martins, L., & de Maio, F. (2021). *European Building Vulnerability Data Repository (v2.1) [Data set]*.

Seismological Survey of Serbia. (2010). *Izveštaj o rezultatima i aktivnostima republičkog seizmološkog zavoda posle zemljotresa644kod kraljeva 03.11.2010 u 01:56 (Report on the results and activites of the seismological survey of Serbia after the earthquake in Kraljevo 03.11.2010 at 01:56)*.

Silva, A., Castro, J. M., & Monteiro, R. (2020). A rational approach to the conversion of FEMA P-58 seismic repair costs to Europe: *Earthquake Spectra*, *36*(3), 1607–1618. https://doi.org/10.1177/8755293019899964

Silva, V., Brzev, S., Scawthorn, C., Yepes, C., Dabbeek, J., & Crowley, H. (2022). A Building Classification System for Multi-hazard Risk Assessment. *International Journal of Disaster Risk Science*. https://doi.org/10.1007/s13753-022-00400-x

Stojadinovic, Z., Kovacevic, M., Marinkovic, D., & Stojadinovic, B. (2017, January). Data-driven Housing Damage and Repair Cost Prediction Framework based on the 2010 Kraljevo earthquake. *Proceedings of the 16th World Conference on Earthquake Engineering (16WCEE)*.

Stojadinovic, Z., Kovacevic, M., Marinkovic, D., & Stojadinovic, B. (2021). Rapid earthquake loss assessment based on machine learning and representative sampling: *Earthquake Spectra*. https://doi.org/10.1177/87552930211042393

Terzic, V., & Kolozvari, K. (2022). Probabilistic evaluation of post-earthquake functional recovery for a tall RC core wall building using F-Rec framework. *Engineering Structures*, *253*, 113785. https://doi.org/10.1016/J.ENGSTRUCT.2021.113785

Underwood, G., Orchiston, C., & Shrestha, S. R. (2020). Post-earthquake cordons and their implications. *Earthquake Spectra*, *36*(4), 1743–1768. https://doi.org/10.1177/8755293020936293

Vamvatsikos, D. (2011). Performing incremental dynamic analysis in parallel. *Computers & Structures*, *89*(1–2), 170–180. https://doi.org/10.1016/J.COMPSTRUC.2010.08.014

Vamvatsikos, D., & Cornell, C. A. (2002). Incremental dynamic analysis. *Earthquake Engineering & Structural Dynamics*, *31*(3), 491–514. https://doi.org/10.1002/eqe.141

Villar-Vega, M., & Silva, V. (2017). Assessment of earthquake damage considering the characteristics of past events in South America. *Soil Dynamics and Earthquake Engineering*, *99*, 86–96. https://doi.org/10.1016/J.SOILDYN.2017.05.004

Wald, D. J., Quitoriano, V., Heaton, T. H., Kanamori, H., Scrivner, C. W., & Worden, C. B. (1999). TriNet "ShakeMaps": Rapid Generation of Peak Ground Motion and Intensity Maps for Earthquakes in Southern California. *Earthquake Spectra*, *15*(3), 537–555. https://doi.org/10.1193/1.1586057

Wang, W. (Lisa), & van de Lindt, J. W. (2021). Quantitative modeling of residential building disaster recovery and effects of pre- and post-event policies. *International Journal of Disaster Risk Reduction*, *59*, 102259. https://doi.org/10.1016/J.IJDRR.2021.102259

World Bank Group. (2020). *Earthquake Risk in Multifamily Residential Buildings, Europe and Central Asia Region*.

Zhang, N., & Alipour, A. (2020). Two-Stage Model for Optimized Mitigation and Recovery of Bridge Network with Final Goal of Resilience. *Transportation Research Record: Journal of the Transportation Research Board*, *2674*(10), 114–123. https://doi.org/10.1177/0361198120935450



This project has received funding from the European Union's Horizon 2020 research and innovation programme under grant agreement No 821115.